UNIVERSITÀ DEGLI STUDI DI TORINO

Doctoral School in Life and Health Sciences

PhD Program in Complex System for Life Sciences

MULTIPARAMETRIC ANALYSIS OF THE ADAPTIVE IMMUNE RESPONSE IN CANCER

Internal tutor:

Prof. Ada Funaro

Candidate:

Valentina Russo

External tutor:

Dr. Luigia Pace

XXXV Cycle

Academic Years: 2019-2022

CONTENTS

ABSTRACT

The immune system plays a critical role in fighting cancer initiation and progression. Tumor infiltrating lymphocytes (TILs), indeed, are an essential component of the tumor microenvironment and have been found to correlate with positive responses to immunotherapy. However, there are still a lot of open questions about TIL heterogeneity and their effector functions following immunotherapy treatment. Understanding lineage relationships between naïve, effectors, memory and exhausted T cell subsets, and the underlying molecular pathways that regulate gene expression programs during the transitions between these distinct states, is essential for the rational design of novel vaccines and the development of new immune-therapeutic protocols. This study aims to examine $CD8^+$ T cell heterogeneity during the different stages of cancer progression, by developing an integrative approach based on the combined analysis of surface markers at protein level and of gene expression profiles at single cell level, in both immunogenic and poorly immunogenic mouse tumor models *in vivo*. The analysis has revealed a complex TIL heterogeneity, with the identification of new subpopulations, among which, transitional memory, $PD1^{low}$ cycling and $PD1^{high}$ exhausted and migratory/exhausted $CD8^+$ T cells. These data have been also validated with neoantigen-specific $CD8^+$ T cells. Taken together these results highlight new interclonal relationships between different $CD8^+$ T subsets in tumors, with distinct self-renewal and functional properties when comparing poorly immunogenic vs immunogenic tumors, and also during the different phases of cancer progression.

INTRODUCTION

The immune system

The immune system is a sophisticated network made up of cells, tissues and organs, which co-operate with the aim of defending the body against harmful dangers, ranging from microbes, like bacteria and viruses, to cancer cells. It plays a crucial role in maintaining the overall health of the body through the recognition and elimination of foreign invaders, while also preventing future infections.

The immune system can be divided into two main branches: the innate and the adaptive immunity. The former acts right after the pathogen invades the organism and provides a non-specific protection against it. This type of immunological defence is exerted by physical barriers, such as the skin and mucous membranes, as well as several types of cells, among which neutrophils, macrophages and natural killer cells head the list. Conversely, the adaptive immunity has a delayed onset, but offers a specific and targeted defence. One of its major advantages is that it can "remember" the first encounter with the pathogen, thus providing long-term immunity against future exposures to the same pathogen (*1*).

The adaptive immunity is mediated by highly specialized cells known as lymphocytes. Furtherly distinguished into B and T cells, they traffic between blood, secondary lymphoid organs and tissues, where they provide protection against a given pathogen or cancer cells. Despite having distinct features and duties, B and T cells share the ability to recognize a molecule, usually a protein, of a given pathogen, commonly referred to as “antigen”.

B lymphocytes

B lymphocytes originate from stem cells present in the bone marrow and their maturation requires several sequential stages, through which they acquire antigen specificity, with the expression of specific surface markers and the formation of the B cell receptor (BCR) (*2*). During this process, autoreactive B cells are eliminated and when mature B cells are formed, they exit the bone marrow and pass to the peripheral lymphoid organs where they can exert their functions. B cells play an important role in both innate and adaptive immunity. According to their localization and function, B cells

can be distinguished into several subsets, namely transitional, follicular B cells, plasmocytes, memory and regulatory B cells.

B cells can be activated by the encounter with their cognate antigen and can release their antigen-specific BCRs, which, in their soluble form, are referred to as antibodies (*3*). They can mediate the humoral immune response via triggering neutralization, opsonisation or complement fixation. Besides antibodies, B cells can also secrete cytokines. Through both the classes of soluble factors, they can influence the behaviour of several cell types, including macrophages, T and dendritic cells.

T lymphocytes

T lymphocytes represents the other branch of the adaptive immune system, exclusively providing cellular-mediated immunity. The precursors of T cells originate in the bone marrow from lymphoid progenitors and differentiate in mature cells in the thymus, where they become able to distinguish self- from non-self-antigens. The specificity in recognizing certain antigens compared to others is given to the T cell receptor (*4*), which arises from the DNA rearrangement during T cell development in the thymus. Each TCR is unique and defines the specificity of each T cell (*5*). Indeed, although all the TCRs have the same structure, constituted by cytoplasmic, transmembrane and extracellular regions, the latter one comprises a variable immunoglobulin-like (V) domain, which is capable of antigen recognition and uniquely characterizes all TCRs. TCR can recognize foreign antigens only if loaded on a heterodimer know as major histocompatibility complex (MHC) exhibited on the surface of other cells. During their development, T cells undergo a process called positive selection (*6*), in order to test their ability of binding with self-MHC. After that, all the T cells that react with self-antigens are eliminated through apoptosis, a process known as negative selection (*7*). During T cell maturation, $CD4^+CD8^+$ thymocytes are generated. CD4 and CD8 are co-receptors that impose restriction on the type of MHC complex that the TCR can recognize and bind. This restriction determines the basis to define the major two T cell subsets. Indeed, $CD4^+CD8^+$ double positive T cells are then selected in order to generate $CD4^+$ or $CD8^+$ single positive cells that migrate to the periphery as naïve T cells. There they can encounter foreign antigens only loaded on MHC. MHC can belong to two distinct classes, namely class I and II. $CD4^+$ and $CD8^+$ T cells will only be able to

recognize a non-self-antigen if duly loaded on MHC-class II and MHC-class I molecules, respectively.

T lymphocytes can be divided in distinct subsets according to their function. A naïve T cell is a cell that has never encountered an antigen so far. Antigen encounter is mediated by cells that exhibit, on their surface, an antigen through a given MHC molecule. When a naïve T cell recognizes a given antigen, it undergoes proliferation and differentiation acquiring several properties. $CD8^+$ T cells mature into cytotoxic $CD8^+$ T lymphocytes (CTL), whereas $CD4^+$ T cells can mature in $CD4^+$ T helper 1 (Th1) or T helper 2 (Th2) cells that are involved in the regulation of both humoral and cellular immunity (Fig. 1.1). After antigen clearance, a small fraction of T cells acquires a memory phenotype and progressively revert to a quiescent state. These cells are responsible in long-term protection (*8*).

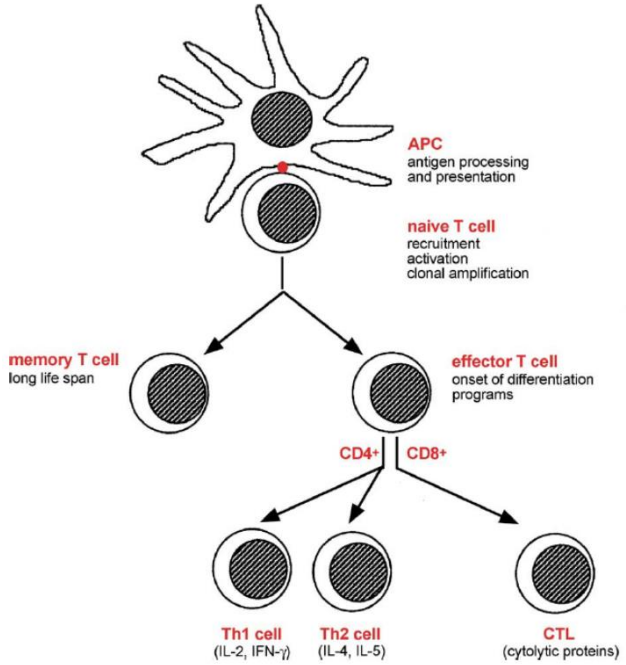

Figure 1.1. Stages of T cell-mediated immune response. Naïve T cells are primed by APC cells and mature in effector T cells. After priming, $CD8^+$ T differentiate in CTL cells, that can directly kill infected cells, whereas $CD4^+$ T cells differentiate in Th1 and Th2 cells that differ in cytokine production. After the elimination of the antigen, a small percentage of cells differentiate in memory T cells. Figure adapted from Fabbri et al., IJBCB, 2003.

$CD4^+$ T cells

$CD4^+$ T cells are involved in both innate and adaptive immunity. They recognize antigens exposed on MHC-II molecules, hence undergoing activation. At this point, they can gain effector properties, secrete various cytokines and migrate to the periphery to activate target cells (*9, 10*). Multiple evidence suggest that $CD4^+$ T cells are very plastic and, in response to microenviromental stimuli, each naïve $CD4^+$ T cell clone can potentially differentiate into distinct subsets (*11*). According to the expression of certain cytokines and specific transcription factors, $CD4^+$ T cells are categorized in five major subsets: Th1, Th2, Th17, T_{REG} and Tfh (follicular T helper) cells. Th1 are involved in fighting intracellular pathogens, tissue repair and antiviral immunity. Th2 cells are accounted to exert defence against extracellular pathogens. $CD4^+$ T cell differentiation towards Th1 or Th2 lineage is strictly depending on specific transcription factors, such as T-bet or GATA-3, and epigenetic modifications (*12*). Th17 cells are mainly known to react against bacteria and fungi. Foxp3-expressing $CD4^+$ T_{REG} cells regulate immune cell homeostasis and prevent excessive an dangerous immunopathology. Tfh cells help B cells produce antibodies.

$CD8^+$ T cells

$CD8^+$ T cell subsets are among the main mediators of the immune system effector function. Naïve $CD8^+$ T cells are activated by recognition of specific peptides presented by the MHC-I on APCs. Once the TCR recognizes the MHC-antigen complex, it engages with a group of membrane proteins known as CD3, whose cytosolic region is responsible for propagating the activation signal. Consequently, $CD8^+$ T cells undergo clonal expansion and differentiation to generate large numbers of effector cells, which are able to enter the blood and migrate into the periphery (Fig. 1.2). This response promotes the acquisition of effector functions, including the expression of cytotoxic proteins, such as perforin and granzyme B, and the production of cytokines, such as gamma interferon (IFN-γ) and tumor necrosis factor alpha (TNF-α) (*13, 14*). The initial activation of naïve $CD8^+$ T cells is associated with the upregulation of specific surface markers, including CD44 and CD69, whereas differentiating effector cells acquire high expression of killer cell lectin-like receptor G1 (KLRG1) and IL-2 receptor subunit-a (CD25), and downregulate the L-selectin (CD62L), the IL-7 receptor subunit-a (CD127) and the CD27 as compared to naive cells.

Following antigen clearance, the majority of effector $CD8^+$ T cells undergo a contraction phase and die by apoptosis. However, a small percentage (5-10%) of them survives and generates long-lived memory T cells, which are preserved in an antigen-independent manner and, upon antigen re-exposure, are able to respond with strong proliferation and rapid conversion into effector cells, which are able to contain a secondary infection (Fig. 1.2) (*15*, *16*).

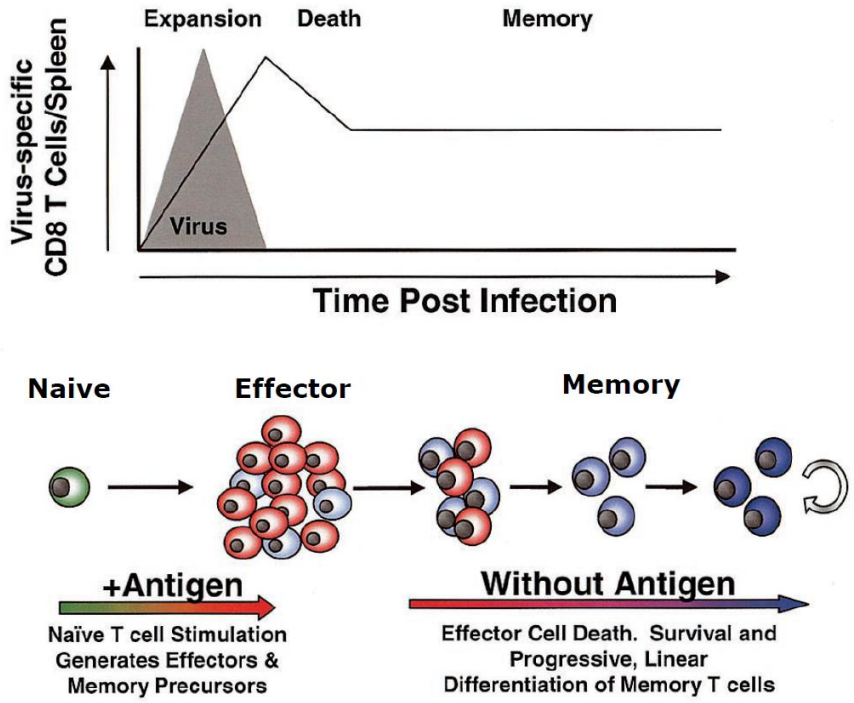

Figure 1.2. Dynamics of $CD8^+$ T cell response to acute infection. After antigen exposure, naïve $CD8^+$ T cells undergo clonal expansion and acquire effector functions. The effector $CD8^+$ T cells are responsible for antigen clearance. The expansion phase is followed by a death phase, when 90% to 95% of the effector T cells die. The surviving $CD8^+$ effector T cells further differentiate giving rise to a memory T cell population that is maintained long term in the absence of antigen via homeostatic turnover. Figure adapted from Wherry, Ahmed, J. Virol., 2004.

Memory potential is not inherited equivalently by all T cells. This means that the process of memory T cells formation is not completely stochastic. As a matter of fact, memory precursor cells can be distinguished from effector cells at early steps of immune responses by high expression of CD44, maintenance of CD127, CD62L, and CD27, and low expression of KLRG1 (*14*).

The differentiation towards a certain fate is associated to transcriptional, epigenetic and metabolic reprogramming and it is depending on environmental stimuli (*17*). At early stages of activation, naïve $CD8^+$ T cells are very plastic, which means they have the ability to generate distinct phenotypes according to different environmental factors (*18*). This potential is lost during clonal expansion and differentiation process towards effector, memory and terminally differentiated T cells.

Memory $CD8^+$ T cell subsets

Immunological memory is one of the most relevant aspects of the immune system. Differently from naïve ones, memory $CD8^+$ T cells can persist in greater numbers (*19*), they can populate peripheral organs (*20*) and, upon antigen re-encounter, they can immediately proliferate and acquire cytotoxic functions (*21, 22*). Furthermore, memory $CD8^+$ T cells are different from the effector ones because they can quickly proliferate after antigen re-exposure and, differently from effectors, they do not undergo contraction but persist in a long-term manner (*23*).

Memory $CD8^+$ T cells make up a heterogeneous group of cells with different phenotypes, tissue localization, self-renewal and protective capabilities. They can differently contribute in maintaining long-term immunity, but their origin and lineage relationship are still not clear. According to this, immunologists have categorized memory T cells into different subsets in order to gain a better understanding on their heterogeneity.

On the basis of the expression of CD62L and CCR7 homing factors, it is possible to categorize memory $CD8^+$ T cells in two main subsets: $CD62L^{high}CCR7^{high}$ central memory (T_{CM}) and $CD62L^{low}CCR7^{low}$ effector memory (T_{EM}) cells (*24*), that together represent the pool of the circulating memory $CD8^+$ T cells. T_{CM} cells are prevalent in secondary lymphoid organs where they persist following infection and can proliferate in response to their cognate antigen (*25*). By contrast, T_{EM} cells have limited expansion potential and are not able to enter lymph nodes from the blood but they express chemokine and integrins for the localization to inflamed tissues and they can rapidly exert effector function upon TCR signalling (*26*). T_{CM} and T_{EM} cells development and functions are characterized by the expression of different transcription factors. Indeed,

T-bet, Blimp1, ID2, and STAT4 expression is associated with T_{EM} cells, while Eomes, TCF1, BCL-6, ID3, and STAT3 expression is associated with T_{CM} cells (*27, 28*).

Tissue surveillance is ascribed not only to T_{EM} cells, but also to a pool of permanent resident cells, known as tissue resident memory T (T_{RM}) cells, that reside within non-lymphoid tissues (*29*). T_{RM} cells are characterized by the expression of CD103 integrin, involved in tissue entry (*30*), and CD69, known to promote tissue retention (*31*), even if the expression level of these markers can be different according to the tissue. T_{RM} cells can also express CXCR3 marker but not CCR7, which both promote T cells to leave non-lymphoid tissues. Transcriptionally, these cells show low expression of T-bet and TCF1 and elevated level of Hobit and Blimp1 (*32, 33*), and their development requires responsiveness to TGF-β (*33, 34*). In line with their role of local sentinels, after antigen reencounter, T_{RM} cells induce a state of inflammation with the production of cytotoxic molecules, such as perforin and granzyme B, cytokines, like IFNγ and TNF, (*35, 36*) and the recruitment of cells belonging to the innate and adaptive immunity (*37, 38*).

Another group of memory T cells, the peripheral memory T (T_{PM}) cells, can be defined on the basis of CX3CR1 expression. Differently from T_{CM}, T_{EM} and T_{RM}, that are $CX3CR1^{-}$, $CX3CR1^{high}$ and $CX3CR1^{-/low}$, respectively, T_{PM} cells express CX3CR1 at intermediate levels ($CX3CR1^{int}$) (*39*). They show the highest self-renewal capacity of all memory T cells and are involved in the peripheral tissue surveillance.

$CD8^+$ T cell exhaustion

$CD8^+$ T cells undergoing persistent antigen exposure can enter a dysfunctional state known as "exhaustion" (Fig. 1.3) (*40*). Persistent antigen stimulation can occur during chronic infections and cancer, when the immune system is not able to effectively eliminate the pathogen or the tumor cells. Key features of T exhaustion are:

- Loss of proliferative capabilities and IL-2 production;
- Loss of effector functions, with reduced production of cytokines, such as IFNγ and TNFα, and consequent impairment of cytotoxic activity (*41*);
- Elevated expression of inhibitory receptors, such as the programmed death-1 receptor (PD-1), Cytotoxic T-Lymphocyte Antigen 4 (CTLA-4), TIM-3, TIGIT and LAG-3 (*42, 43*). These receptors are expressed at low levels also on effector $CD8^+$ T cells and represent checkpoints that prevent immune cells from destroying

healthy cells and from causing autoimmune reactions. They interact with their ligands on cells exhibiting a given MHC-antigen complex, leading to a consistent reduction of T cell activation and effector functions (*44*);

- Transcriptional and epigenetic changes with the downregulation of genes involved in T cell activation.

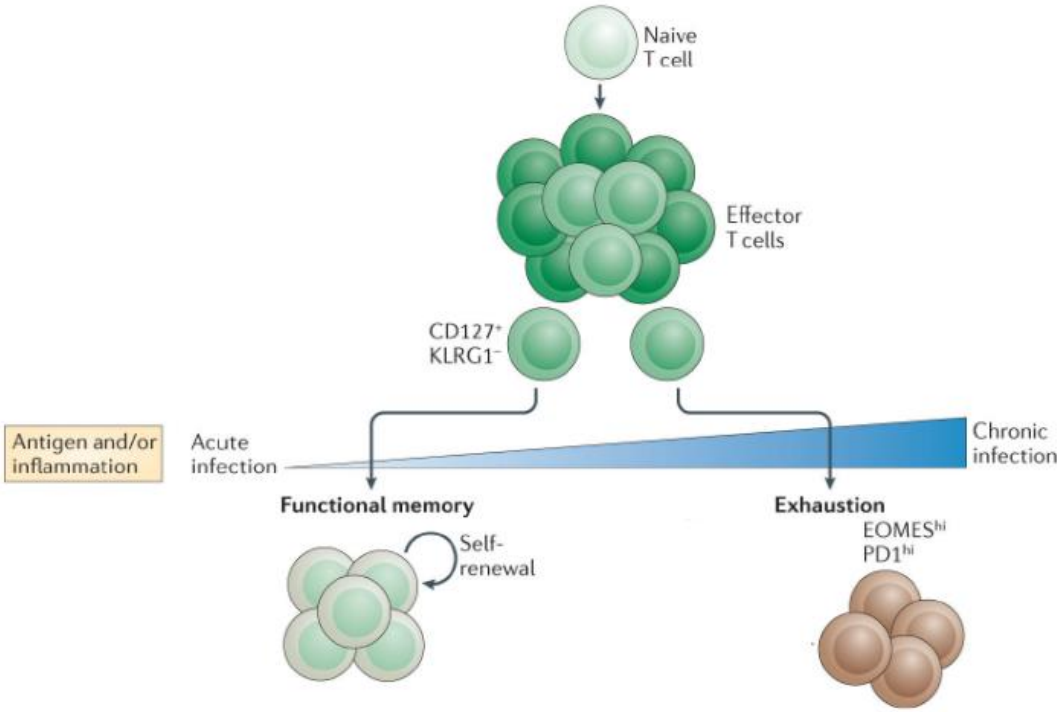

Figure 1.3. T cell exhaustion development. Naïve T cells are activated by their cognate antigen and proliferate to generate effector cells. The majority of effector $CD8^+$ T cells undergo contraction, whereas a small fraction of $CD127^+KLRG1^-$ T cell can either differentiate into memory or dysfunctional $CD8^+$ T cells. During acute infection, after antigen clearance, effector $CD8^+$ T cells differentiate into functional memory $CD8^+$ T cells with self-renewal capabilities. On the contrary, during chronic infection or cancer, with persistent T cell stimulation, effector $CD8^+$ T cells become exhausted. Figure adapted from Wherry et al., Nat Rev Immunol, 2015.

The main driving force of T cell exhaustion establishment is the continuous exposure to the antigen, but additional factors can contribute to exhaustion, such as the lack of CD4 T cell help (*45*) or direct signals from the inhibitory receptors (*46*). Several studies demonstrate that the severity of exhaustion also depends on the level of antigen stimulation (*41, 47, 48*). Furthermore, IL-10 and TGFβ suppressive cytokines or immune cells, such as $Foxp3^+CD4^+$ regulatory T cells (*40*), are accounted as responsible of T cell exhaustion maintenance.

Among the aforementioned checkpoints, PD-1 is the most associated with T cell exhaustion (*49, 50*). It is not expressed by naïve T cells but undergoes upregulation during T cell activation. If the antigen is cleared, PD-1 levels decrease. On the contrary, when there is a persistent antigen exposure, PD-1 expression remains high, indeed several epigenetic modifications occur on in the *pdcd1* locus, leading to the durable expression of PD-1 on antigen-specific T cells (*51*). PD-1 can control the exhausted state by directly influencing T cell functional properties, for example repressing TCR signaling (*52*), or by inducing paralysis of T cell motility (*53*).

In addition, in the context of cancer, during T cell exhaustion, the expression of the inhibitory receptors increases and cancer cells can take advantage of this by overexpressing ligands to escape the immune response. This knowledge has brought to the design of cancer immunotherapies based on the employment of antibodies as inhibitors of these immune checkpoint receptors (*54*). For example, the blockade of the PD-1/programmed death-ligand 1 (PD-L1) pathway suppresses tumor growth restoring some functions of the exhausted cells (*42*). From this, it arouse the doubt that exhausted T cells are not completely terminally differentiated cells and that exhaustion might be a reversible state. Indeed, exhausted $CD8^+$ T cells are a very heterogeneous population, within which it is possible to distinguish at least two main subsets. T-bet^{high}PD-1^{int}$CD8^+$ T cells are accounted as progenitor exhausted cells, whereas Eomes^{high}PD-1^{high}$CD8^+$ T cells as terminally differentiated exhausted cells, which exhibit low proliferative capabilities and higher expression of inhibitory receptors when compared to their progenitors (*55*). Overtime, with antigen persistence, progenitors are lost and Eomes^{high}PD-1^{high}$CD8^+$ T cells accumulate. These two populations show a different responsiveness to the blockade of PD-1 pathway: exhausted T cells, expressing intermediate levels of PD-1, are converted to non-exhausted through PD-1 blockade, whereas PD-1^{high} exhausted cells cannot (*56*) (Fig. 1.4).

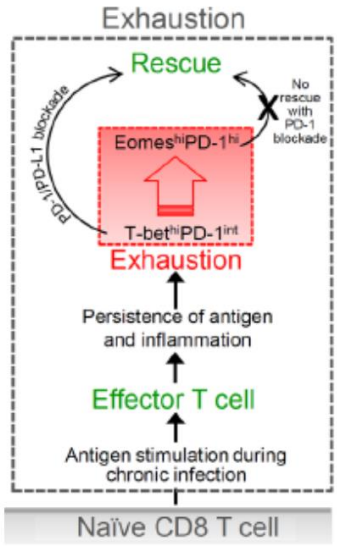

Figure 1.4. T cell exhaustion reversibility. During chronic infection, persistent antigen stimulation determines progressive T cell differentiation towards exhaustion. In this context, Tbet^{high} PD-1^{int} but not Eomes^{high} PD-1^{high} exhausted T cell functionality can be reversed by PD-1 blockade. Figure adapted from Schietinger et al., Trends Immunol, 2014

Tumor antigenicity and immunoediting

The interaction between the immune system and cancer is crucial for the control of tumour development and progression. Indeed, during the early stages of tumor development, immune cells can control the growth of cancer cells. This is possible because tumor cells express antigens that distinguish them from healthy cells (*57*). Tumor antigens can be grouped in two categories: tumor-specific antigens (*58*) and tumor-associated antigens (TAAs) (*59*). TSAs, also called neoantigens, are oncogenic or abnormal proteins that arise from somatic alterations. These antigens are not encoded in normal cells but only in tumor ones, and for this reason they are accounted as foreign proteins by the immune system. On the contrary, TAAs are self-antigens encoded by unmutated genes, but they are abnormally expressed in tumor cells compared to normal cells. Differently from TSAs, visible targets for the immune system, TAAs are more susceptible to immunological tolerance (*60*, *61*). Aberrant tumor antigens can be presented by MHC molecules on the cell surface and subsequently they can be recognized by T cells. Following activation, CD8$^+$ T cells infiltrate the tumor and attack the transformed cells by producing antitumor cytokines and cytotoxic molecules, such as interferon-γ (IFNγ), tumor necrosis factor-α (TNFα), perforin, and granzymes (*62*). These activated T cells are called tumor infiltrating lymphocytes (TILs) and are a

heterogeneous group of lymphocytes that differ in their capability to enhance the anti-tumor immune responses (*63*). TILs have been detected in tumor tissue, tumor-associated lymph nodes and metastases of several cancers and they are associated with better prognosis in almost all types of tumors. However, the antitumor effect of the TILs is transient, because overtime the tumor develops mechanisms to evade the immune system. As a matter of fact, the immune system can both protect the host and promote the tumor development by shaping its immunogenicity. This concept is well expressed by the cancer immunoediting hypothesis that includes three phases: elimination, equilibrium and escape (*64*). During the elimination, the immune system recognizes and destroys the tumor but some transformed cells can survive and become immune-resistant. Hence, an equilibrium state can be established between the tumor and the immune system. In this phase, potentially considered the longest one, the immune system controls the cancer cells, but it is not able to destroy them. Progressively, the continuous selection of immune-resistant cells can lead to the complete escape of the tumor from the immune response (*64*) (Fig. 1.5).

In this context, during cancer immunoediting, tumor cells can evolve and avoid TILs-mediated elimination. This is possible thanks to different mechanisms, such as the loss of antigenicity, the loss of immunogenicity or the establishment of an immunosuppressive microenvironment (Fig. 1.6). Antigenicity loss can happen when cancer cells lacking mutated immunogenic antigens are positively selected by the immune system or in case of loss of the MHC, incompatible with antigen presentation and immune system activation. Tumor antigenicity is strictly connected to immunogenicity, defined as “the ability of a molecule or a substance to provoke an immune response”. When a tumor undergoes loss of antigenicity, also its immunogenicity is compromised and cancer cells become “invisible” to the immune system.

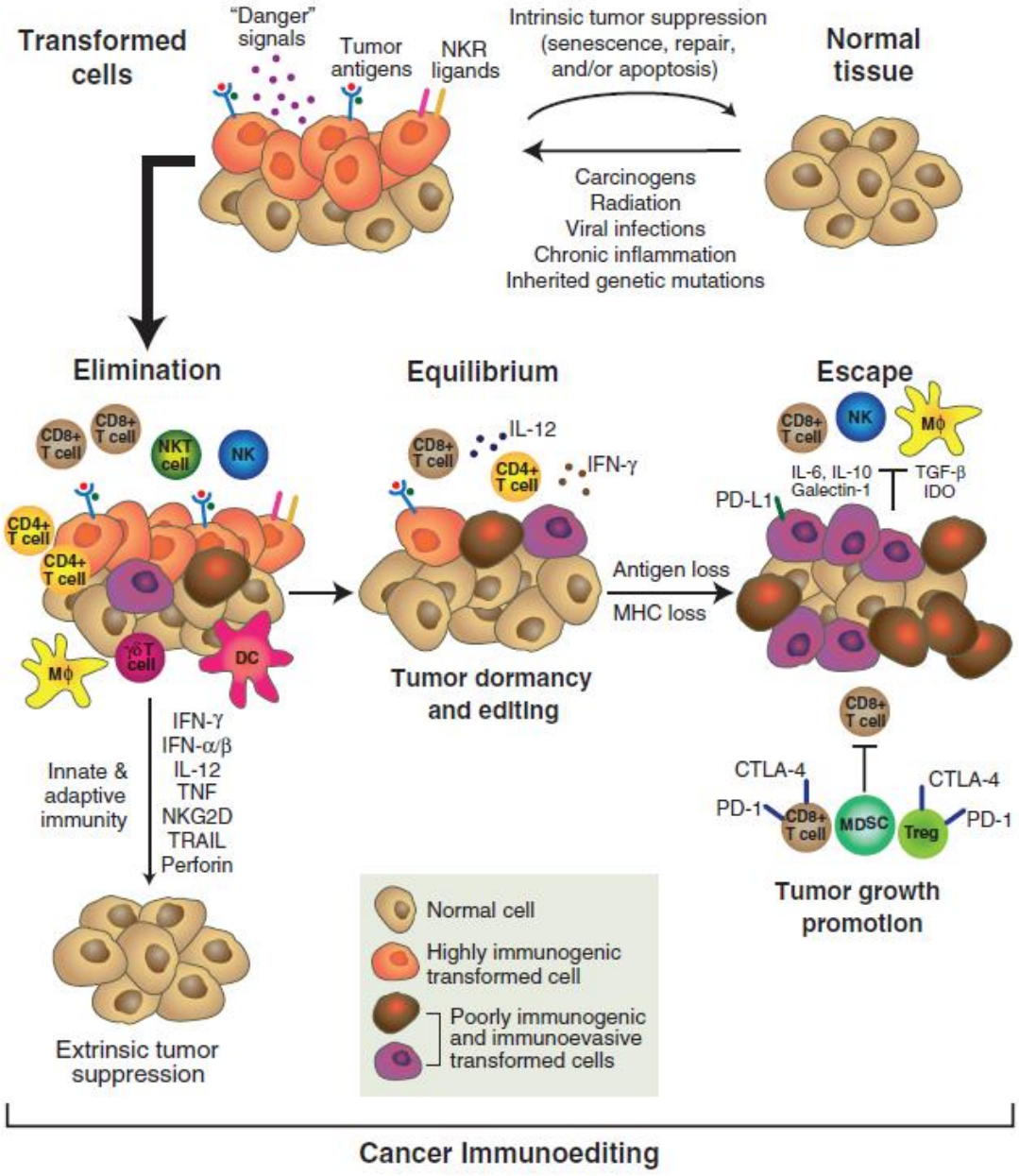

Figure 1.5. Cancer immunoediting concept. Cancer immunoediting consists of three states: elimination, equilibrium and escape. During the elimination, the innate and adaptive immunity try to eradicate cancer cells before they become clinically detectable. If the elimination phase fails, it enters a situation of equilibrium in which tumor growth is still under control. At this stage, immune system can both protect against cancer initiation as well as edit its immunogenicity leading to the tumor progression. Figure adapted from Vesely et al., Annu. Rev. Immunol, 2011.

Escape can also occur because of the establishment of an immunosuppressive microenvironment. In this case, cancer cells can produce immunosuppressive cytokines,

such as the vascular endothelial growth factor (VEGF), which stimulates tumor growth through the promotion of angiogenesis, or the transforming growth factor-β (TGF-β) (*65*). Moreover, in order to evade the immune system, tumors can promote the recruitment of T_{REG} cells (*66*), which inhibit T cells function through the secretion of IL-10 or TGF-β or through the upregulation of the expression of negative co-stimulatory molecules, such as the PD-L1 or CTLA-4 that can induce $CD8^+$ T cell exhaustion (*40*).

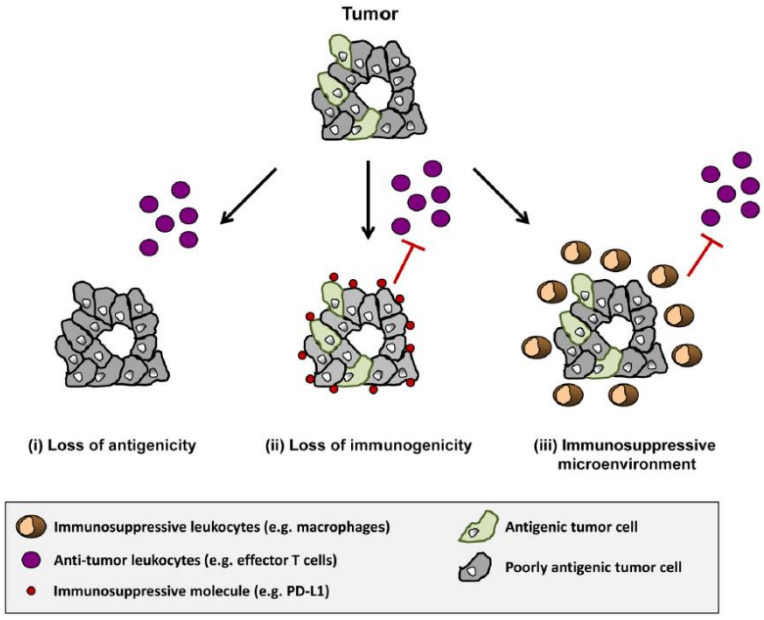

Figure 1.6. Immune escape in cancer. There are three mechanisms by which tumor immune escape can arise. The first one is the loss of antigenicity, that can happen because of defects in the antigen processing and/or presentation. The second one is the loss of immunogenicity, that can be caused by the positive selection of tumor cells expressing antigens that elicit a weak immune response. The last one is the establishment of an immunosuppressive microenvironment defined by the tumor cells themselves and by the recruitment of cells with immunosuppressive properties. Figure adapted from Beatty et al., Clin Cancer Res, 2016.

TILs

Tumor microenvironment consists of cancer cells, but also endothelial cells, stromal fibroblasts and infiltrating leukocytes, such as dendritic cells, macrophages and lymphocytes (*67*). TILs, that include different cellular types, such as $CD3^+$, $CD4^+$, $CD8^+$ lymphocytes and T_{REG} cells, are defined as lymphocytes that surround the tumor and can control cancer progression. They have been found in different solid cancers, such as

colorectal, ovarian and lung tumors (*68*) and they are usually associated to a better prognosis and survival (*69, 70*). TIL infiltrate can be classified according to its extent and density as: absent, non-brisk or brisk (*71*). In the first case, lymphocytes are not present or they are in the periphery of the tumor without infiltrating it. Non-brisk infiltrate is so defined when TILs are present only focally, whereas when they are located along the entire base of the tumor the infiltrate is considered brisk. Recent studies demonstrated that beyond TILs density also their spatial organization can impact on prognosis. For instance, a high TIL infiltrate localized at the invasive tumor margin has a better positive correlation with overall survival and disease-free survival when compared with TIL infiltrating the centre of the tumor (*72, 73*). Moreover, many studies demonstrate that some TILs can be associated to a better prognosis compared to others. For example, $CD8^+$ TILs are associate with more favourable prognosis respect to $CD3^+$ or $CD4^+$ T cell infiltrates (*74, 75*). In this context, substantial improvement has been made in the identification of prognostic value and, beyond classical CD3, CD4 and CD8, also other markers, such as CD103 or PD-1, can be considered in the assessment of cancer prognosis (*76, 77*). CD103 is encoded by *ITGAE* gene and is a transmembrane heterodimeric protein involved in cell adhesion, migration and lymphocyte homing though the interaction with E-cadherin (*78*), that is expressed in epithelial cells. Intratumoral $CD8^+CD103^+$ TILs strongly correlate with increased overall survival in several type of cancer with epithelial origin, such as ovarian, breast, colorectal, head and neck cancer (*79-83*). PD-1 is a marker of exhaustion expressed both on $CD4^+$ and $CD8^+$ T cells. There are contrasting evidence about the association of this marker to a positive or negative prognostic value. Indeed, some studies in nasopharyngeal carcinoma showed lower overall survival related to PD-1 expression (*84*), whereas studies in non-small-cell lung cancer (NSCLS) reported a positive correlation with the presence of $PD\text{-}1^+$ cells in the tumor infiltrate (*85*). These results suggest that evaluation of PD-1 as prognostic value depends not only on its presence but it is also associate to the tumor type.

Cancer immunotherapy

Cancer cells can escape the immune system by several mechanisms, among which loss of antigenicity or the establishment of an immunosuppressive microenvironment. The

degree to which a tumor is able to become "invisible" to the immune system can vary from one type of cancer to another and several efforts have been made in order to define strategies to restore immunosurveillance in cancer. These strategies can be resumed in three main goals: modulate tumor inflammation, induce or boost T cell anti-tumor immunity and reverse the mechanisms of immune tolerance. According to this, different form of immunotherapies have been developed to reach this aim and they can be grouped in: oncolytic virus therapies, cancer vaccines, cytokine therapies, adoptive cell transfer (ACT) and immune checkpoints inhibitors (Fig. 1.7).

Oncolytic virus therapies exploit the ability of some virus to infect and kill tumor cells directly or by the establishment of a proinflammatory environment that can trigger the immune response (*86*). One oncolytic virus approved by the Food and Drug Administration (FDA), known as talimogene laherparepvec (T-Vec), is a genetically modified herpesvirus for the treatment of metastatic melanoma (*87*).

Cytokines are signalling proteins involved in several processes, such as growth, differentiation, pro-inflammatory and anti-inflammatory systems. Several cytokines can reduce cancer cell growth by exerting direct pro-apoptotic and anti-proliferative activity or by indirect stimulation of cytotoxic lymphocytes. Two cytokines, IL-2 and IFN-α, have been approved by the FDA for several tumors. IL-2 was approved for the treatment of metastatic melanoma (*88*) and renal cell carcinoma (*89*), while IFN-α was approved for the treatment of follicular non-Hodgkin lymphoma (*90*), hairy cell leukemia (*91*) and melanoma (*92*). However, the half-life of these cytokines is short, their action is limited and leads to a low response rate. Thus, this therapy is usually not preferred compared to immune checkpoint inhibitors or targeted therapy.

ACT relies on the use of patient's own TILs to eliminate cancer cells. Indeed, the TILs can be isolated, expanded *in vitro* and reinfused back into the patient with appropriate growth factors able to stimulate their survival (*93, 94*). ACT can be classified in: ACT with TIL (*93*), with T-cell receptor-engineered T cells (*95*) and with chimeric antigen receptor (CAR)-T cells. In ACT with TCR-engineered T cells, T cells can be modified to express TCR targeting specific tumor antigens (*96*). However, the loading of the processed antigen on the MHC is necessary for it recognition by the TCR, and one of the mechanism of tumor escaping from the immune system is the downregulation of MHC. To overcome MHC restriction, CAR molecules have been developed (*97*). CARs

are hybrid receptors that utilize antibody fragments to recognize specific antigens expressed on the surface of cancer cells and CD19-specific CAR-T cells are successfully employed in several haematological tumors (*98*).

Another category of cancer immunotherapy is represented by the immune-checkpoint inhibitors. CTLA-4 and PD-1 are co-inhibitory receptors that hamper unwanted activation of the immune system. It is well known that the tumor cells can take advantage of this to escape the immune system. Indeed, when T cells are activated by the recognition of tumor-specific antigens, cancer cells sense they are attacked by recognizing IFN-γ produced by T cells themselves and upregulate the expression of PD-L1. Blockade of this pathway with antibodies allows to induce T cell cytotoxic activity. Clinical immunotherapies with monoclonal antibodies blocking PD-1 or its ligand PD-L1 and CTLA-4 have been approved for the treatment of melanoma, Hodgkin lymphoma and NSCLS (*54, 99, 100*).

Cancer vaccines aim to kill tumor cells by antigen-specific immune response. The success of this type of immunotherapy depends on the type of antigens that should be expressed only by tumor cells, the tumor microenvironment and the formulation of the vaccine itself. Indeed, based on the different preparation methods cancer vaccines are divided into four categories: cell based vaccines, that use cell as antigen carrier (*101*), viruses-based vaccines, that use a virus as vectors (*102*), peptide-based vaccines (*103*), and nucleic acids-based vaccines, that include DNA or RNA encoding genes of pathogenic antigens (*104*).

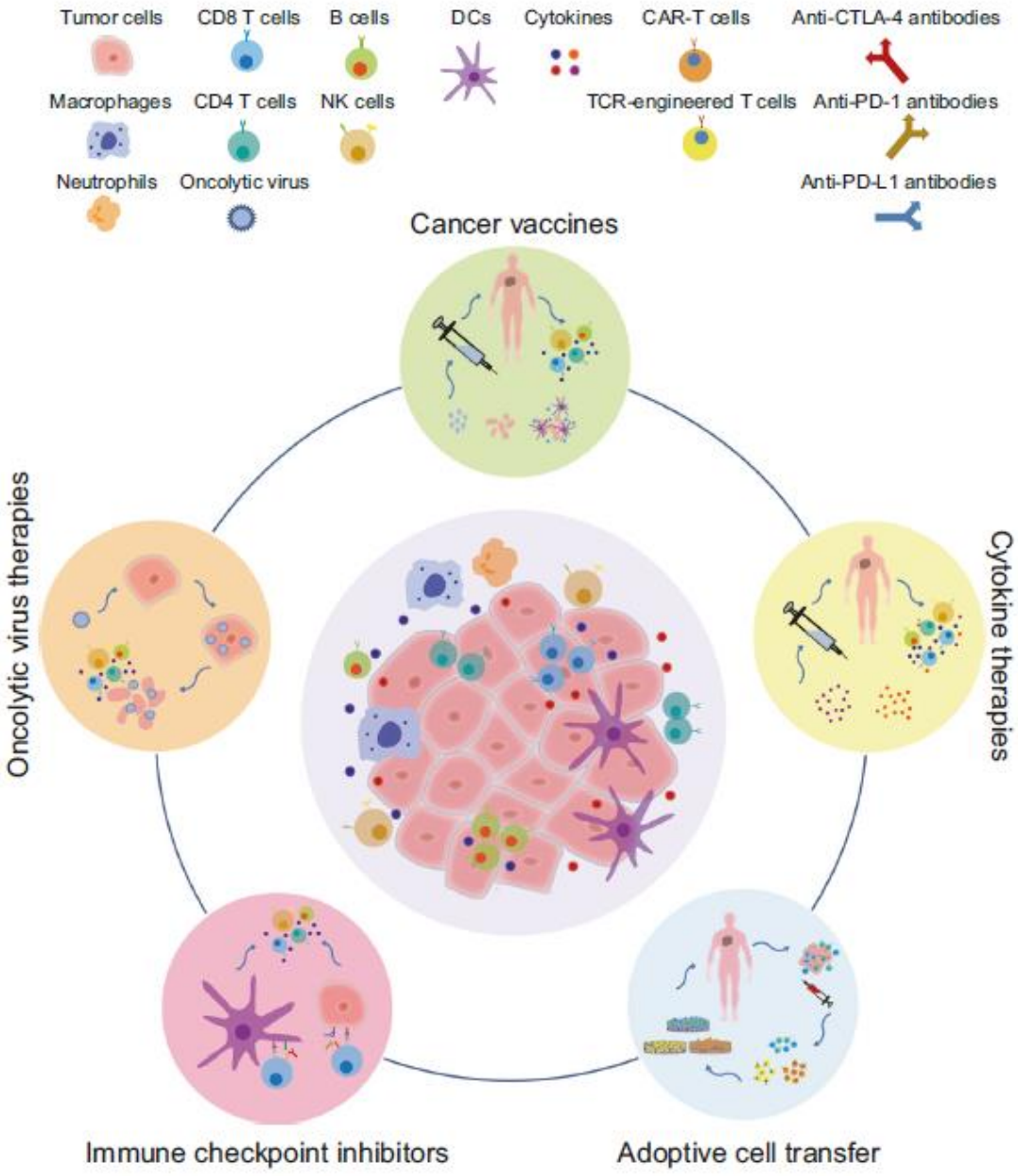

Figure 1.7. The major categories of cancer immunotherapies. Different forms of cancer immunotherapy, including oncolytic virus therapies, cancer vaccines, cytokine therapies, adoptive cell transfer, and immune checkpoint inhibitors, have evolved. Figure from Zhang et al., Cellular and Molecolar Immunology, 2020.

AIMS

TILs are the frontline soldiers of the adaptive immune system and are recruited into the tumor microenvironment to fight cancer development and progression. Understanding the mechanisms of $CD8^+$ T cell differentiation in correlation with cancer progression or control is fundamental for the development of new immunotherapeutic approaches.

The major objectives of this project are:

1. to study $CD8^+$ TIL heterogeneity taking advantage of a multi-omic technique that allows the combined analysis of transcriptome and proteome at single cell level;

2. to investigate T cell responses during tumor growth in different murine cancer models, with particular focus on the analysis of different $CD8^+$ T cell subpopulations (identified above) with a critical role in immune response during cancer progression;

3. to analyse $CD8^+$ T cell differentiation in highly and poorly immunogenic tumor models in order to identify $CD8^+$ T cell subpopulations that positively correlate with tumor control or rejection.

RESULTS

Analysis of $CD4^+$ and $CD8^+$ T cells by single-cell multi-omics approach

To study TIL heterogeneity, we relied on a single-cell multi-omics approach, based on the BD Rhapsody single-cell analysis. This system is based on the combined analysis of transcriptome and surface protein expression. Lymphocytes heterogeneity is usually defined according to the surface marker expression predicted by the gene expression profile, but often there isn't a strong correlation between transcriptome and proteome (*105, 106*). Consequently, BD Rhapsody single-cell analysis, which integrates genes and surface markers expression, allows to overcome this limit.

The experimental design used in our study is schematically represented in Fig. 2.1A. C57BL/6 mice were subcutaneously (s.c.) injected with MC38 murine colon cancer cells and they were sacrificed after 20 days to collect tumors (Tm) and draining lymph nodes (dLNs). Following lymphocytes isolation and surface marker staining, $CD4^+$ and $CD8^+$ T cells were sorted, they were labelled with Sample Tag and Ab-O, and loaded on BD Rhapsody System (Fig. 2.1B). Sc-RNA and sc-Ab-O libraries were then generated and sequenced (*107*).

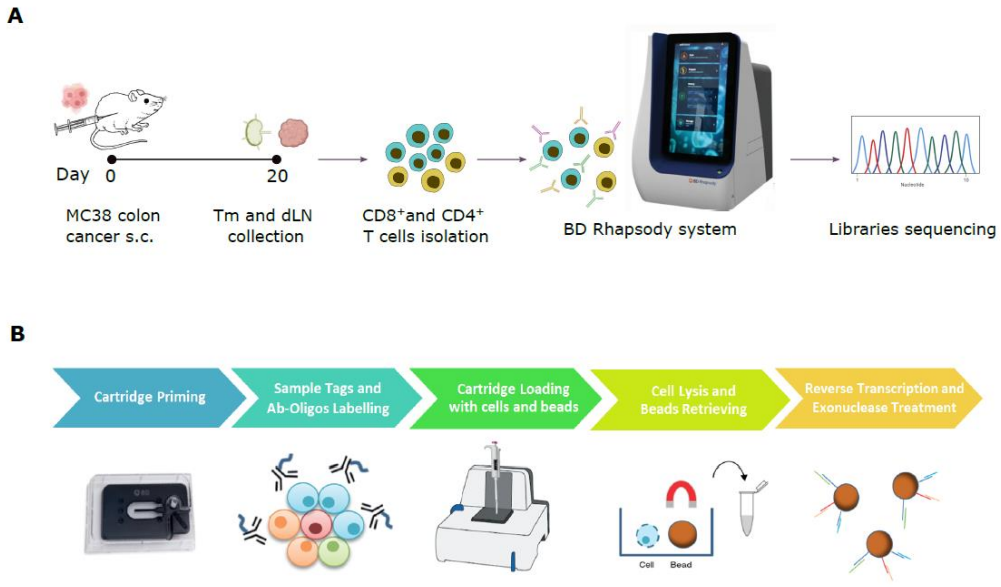

Figure 2.1. Experimental design and BD Rhapsody single-cell analysis system workflow. (**A**) C57BL/6 mice were subcutaneously (s.c.) injected with MC38 colon carcinoma cells. After 20 days, tumors and draining lymph nodes were collected and lymphocytes isolation was performed. Cells were labelled with antibodies against specific surface markers and processed in order to generate single-cell libraries by BD Rhapsody system. (**B**) After cartridge priming

and cell labelling with Ab-O and Sample Tag, cells and beads were loaded on the cartridge. Then, cell lysis was performed in order to hybridize the mRNA and Ab-O onto the beads. During the retrieval step, the beads were recovered and ready for reverse transcription and exonuclease I treatment. Figure adapted from Russo et al., Methods Mol Biol, 2022.

Thanks to the use of different Sample Tags, we were able to discriminate the TILs and the lymphocytes derived from the dLNs. We observed that cells belonging to the same tissue grouped together, suggesting that the environment strongly influence cell gene expression (Fig. 2.2A). The distribution of CD4 and CD8 markers is shown in Fig. 2.2B. Other markers, such as naïve or effector and exhaustion markers, showed a different distribution between the dLNs and the tumors. Indeed, CD62L and CCR7, which are markers of naïve cells, were more expressed among lymph nodes cells compared to TILs, whereas activation and exhaustion markers such as CD44, CD69, CD25 and TIM-3 were more represent among TILs (Fig. 2.2C).

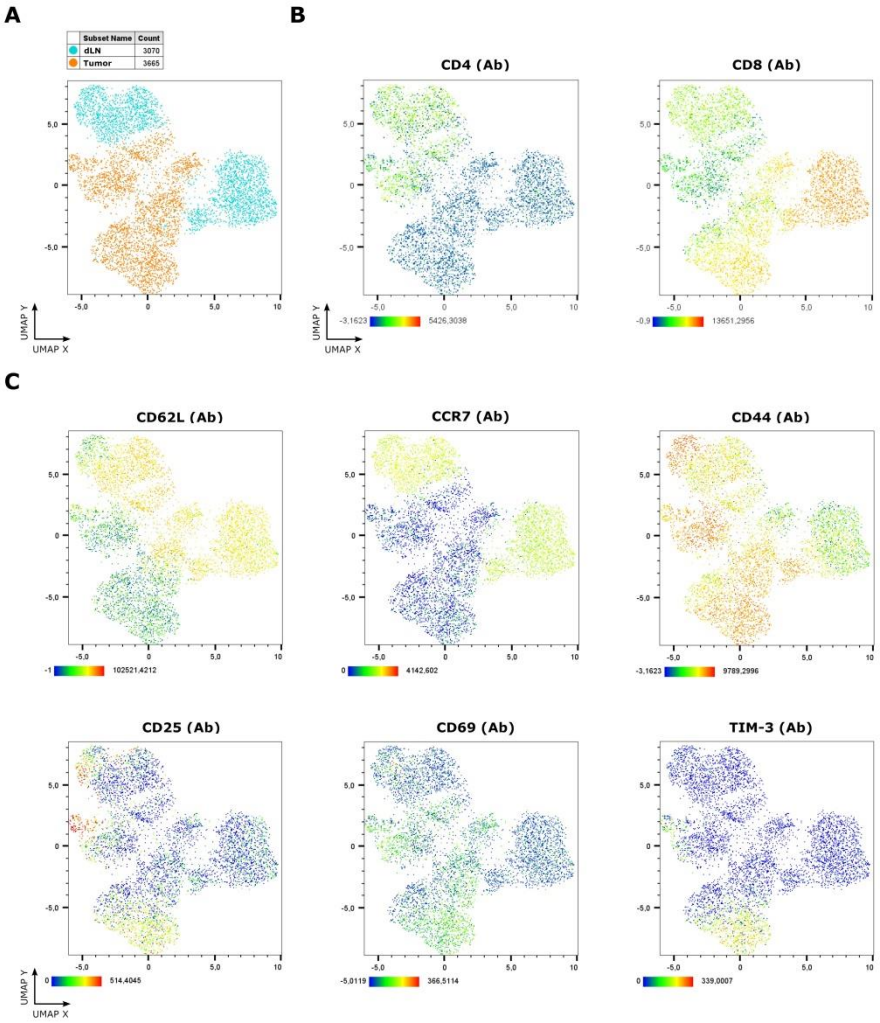

Figure 2.2. Single-cell data from tumor and dLN compartments. (**A**) UMAP projection of data showing tumor and dLN cells stained with different Sample-Tag. (**B-C**) UMAP projections with cells coloured according to the expression levels of CD4, CD8 (**B**), naïve and effector/ exhausted surface markers, such as CD62L, CCR7, CD25, CD69, CD44 and TIM-3 (**C**). Each dot represents a single cell.

In order to analyse T cell subsets in dLNs and tumors, we performed clustering analysis using the Phenograph algorithm, which partitions high-parameter single-cell data into phenotypically distinct subpopulations (*108*). According to this, we were able to identify twelve non-overlapping distinct clusters between TILs and lymphocytes from dLNs (Fig. 2.3A).

Among the $CD4^+$ T cells we distinguished six clusters, three of which belonging to the dLNs and three among the TILs (Fig. 2.3B, left). In dLNs we identified two clusters of naïve T cells (N1 and N2 $CD4^+$_dLN) expressing high levels of CCR7 and CD62L but low levels for the activation markers, such as CD44, and one cluster of regulatory T cells (T_{REG} $CD4^+$_dLN), defined based on the expression of CD25 and GITR (Fig. 2.2C and 2.4A). $CD4^+$ T_{REG} cells (T_{REG} $CD4^+$_Tm) were also identified among TILs. In the tumors, we defined one cluster of early activated cells (EA $CD4^+$_Tm) and one cluster of effector cells (T_{EFF} $CD4^+$_Tm).

Among $CD8^+$ T cells, we identified six different clusters, only two of which belonging to dLNs (Fig. 2.3B, right). We classified one cluster derived from dLNs as $CD8^+$ naïve cells (N $CD8^+$_dLN) because they highly expressed naïve markers, such as CD62L and CCR7, while showing low expression of the CD44 activation marker (Fig. 2.2C and 2.4A). The second cluster was defined as $CD8^+$ central memory cells (T_{CM} $CD8^+$_dLN) since they showed high levels not only of CD62L and CCR7, that are considered lymph nodes homing receptors, but also of CD122, known as a memory marker (Fig. 2.2C and 2.4A).

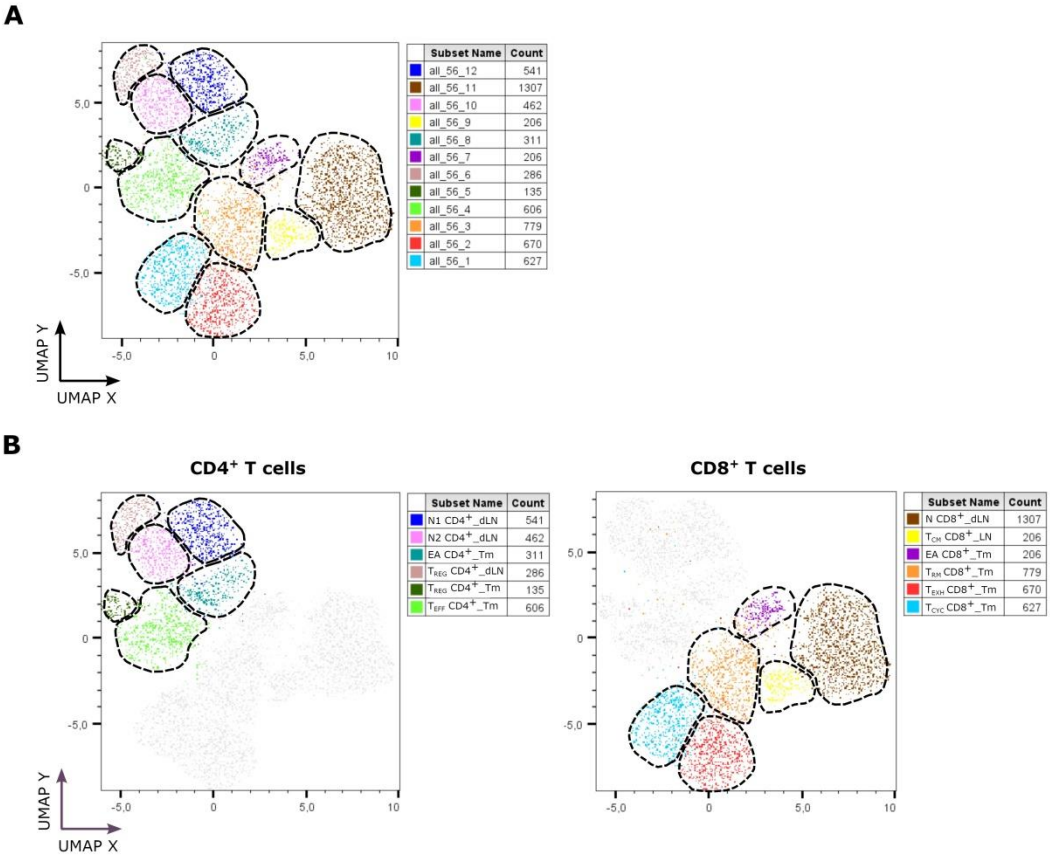

Figure 2.3. Clustering analysis. (**A**) UMAP projections of the twelve clusters identified by integrating both transcriptomic and proteomic data. (**B**) UMAP projections of the clusters identified in the $CD4^+$ (left) and $CD8^+$ (right) compartments. Each dot represents a single cell. N: Naïve, EA: Early Activated, T_{REG}: T regulatory, T_{EFF}: T effector, T_{CM}: T central memory, T_{RM}: Tissue resident memory, T_{EXH}: T exhausted, T_{CYC}: T cycling.

When we analysed TILs, we identified one cluster of exhausted T cells (T_{EXH} $CD8^+$_Tm) expressing high levels of immune-checkpoint inhibitor markers, such as LAG-3, PD-1, TIM-3 and TIGIT (Fig. 2.4A). Another cluster was classified as cycling cells (T_{CYC} $CD8^+$_Tm), because of the upregulation of genes associated to the proliferation, such as *Birc5*, *Mcm4*, *Mcm5 and Mki67* (Fig 2.4B).

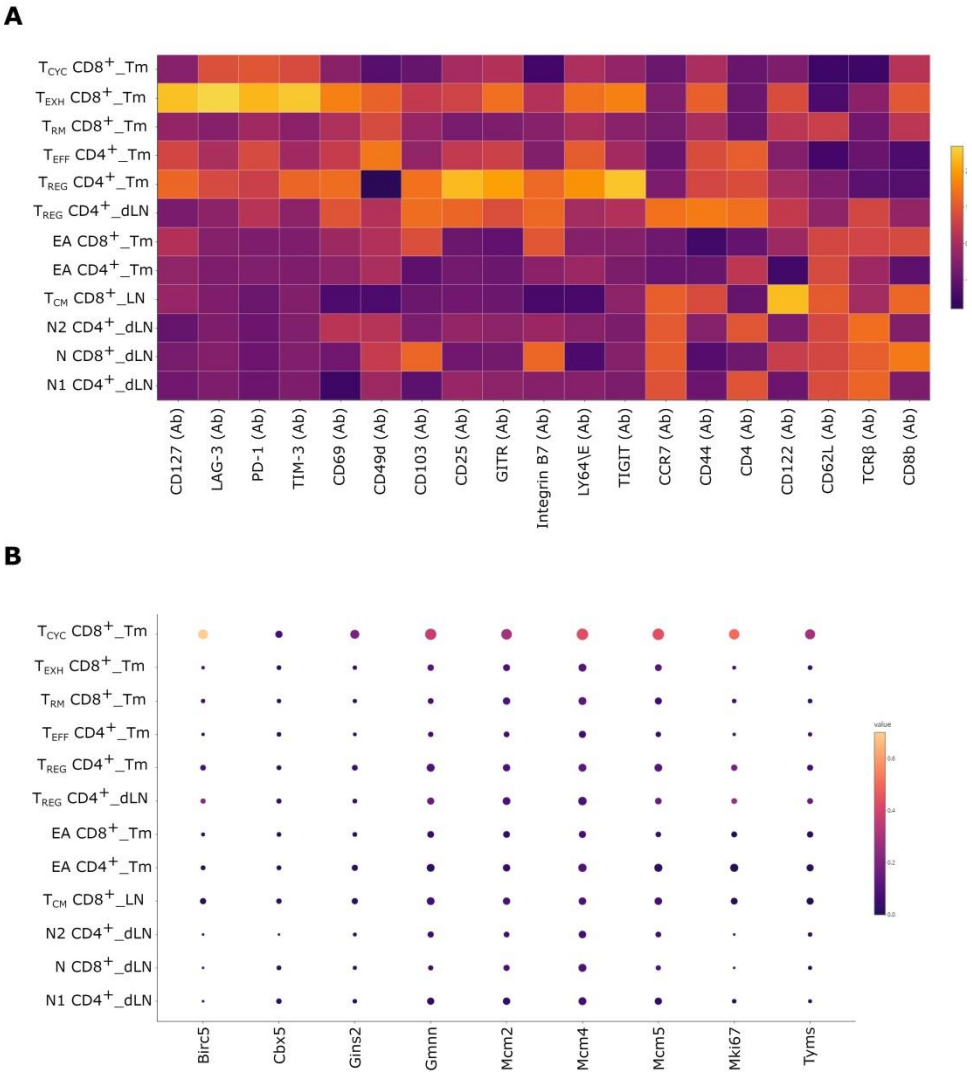

Figure 2.4. Surface markers and cell cycle-related genes distribution. (**A**) Heatmap showing the distribution of some surface markers used to define clusters immune phenotype. (**B**) Bubble heatmap showing the distribution of cell cycle-related genes used to define clusters. N: Naïve, EA: Early Activated, T_{REG}: T regulatory, T_{EFF}: T effector, T_{CM}: T central memory, T_{RM}: Tissue resident memory, T_{EXH}: T exhausted, T_{CYC}: T cycling.

The third cluster was characterized by $CD69^{+}$ and $CD103^{low}$ cells, suggesting they could represent tissue resident memory cells (T_{RM} $CD8^{+}$_Tm) (Fig. 2.5A). In particular, we observed that the expression of other markers, such as CD62L and CD49d, was quite heterogeneous, as they could be associated to different phenotypes. Indeed, this cluster could be further divided into different subpopulations. For example, we could distinguish one subset of $CD62L^{low}$ $CD49d^{high}$ $CD8^{+}$ $PD\text{-}1^{low}$ T_{RM} cells and one subset of $CD62L^{high}$ $CD49d^{low}$ $PD\text{-}1^{low}$ $CD8^{+}$ T_{RM} cells (Fig. 2.5B-C). Moreover, we could also

identify a group CD62L^{high}CD49d^{high} cells with downregulated CD103 expression when compared to the other two clusters (Fig. 2.5C).

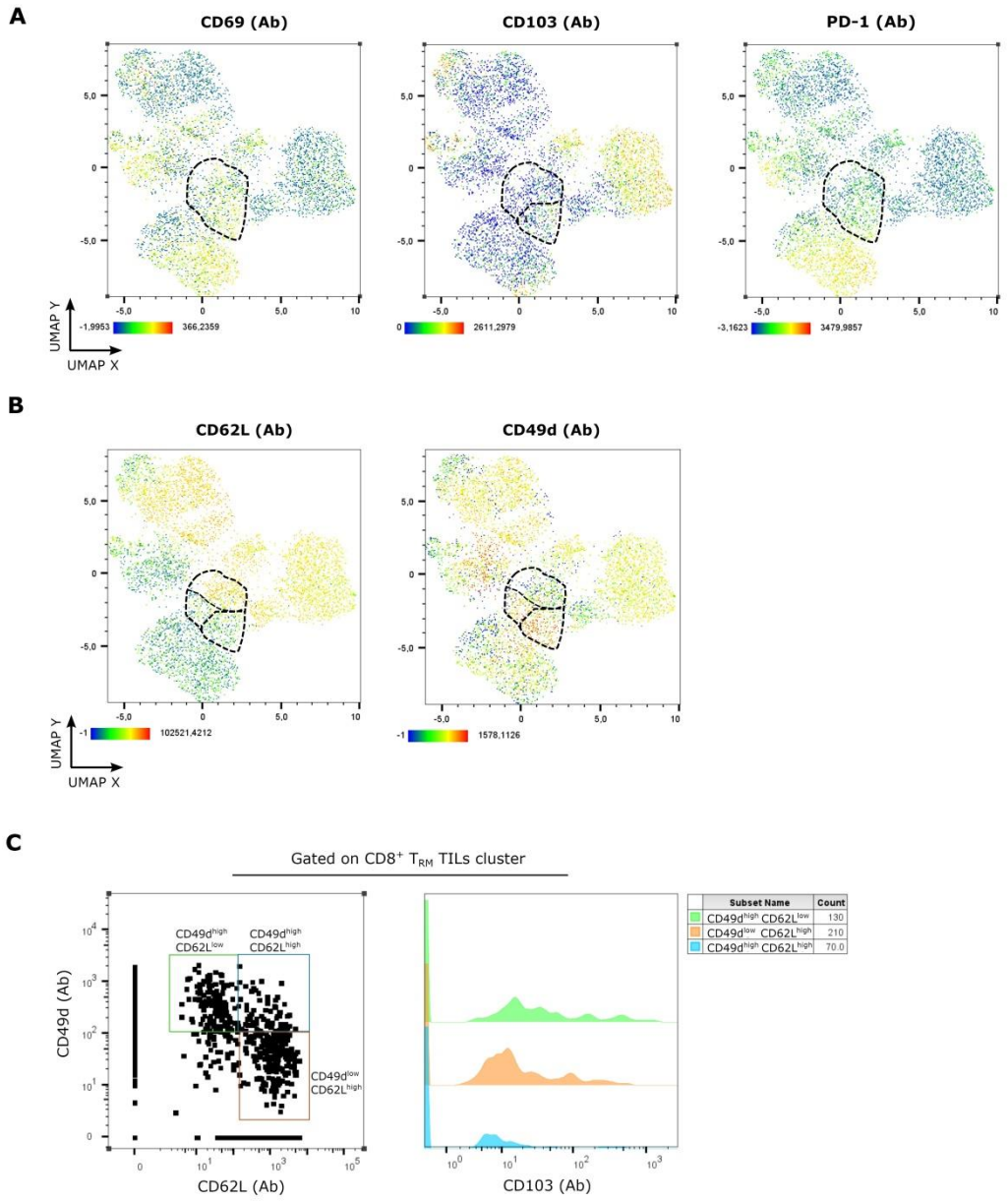

Figure 2.5. Surface markers distribution in T_{RM} cell cluster from tumors. (**A-B**) UMAP projections showing cells coloured according to the expression levels of CD69, CD103, PD-1 (**A**), CD62L and CD49d (**B**) surface markers, with focus on T_{RM} cluster from tumors. (**C**) Dotplots showing CD49^{high}CD62L^{low}, CD49d^{low}CD62L^{high} and CD49d^{high}CD62L^{high} cells gated on T_{RM} cluster from tumors (left panel). Histograms showing CD103 expression in CD49^{high}CD62L^{low}, CD49d^{low}CD62L^{high} and CD49d^{high}CD62L^{high} T_{RM} cells from tumors are also reported (right panel). Each dot represents a single cell.

Finally, we identified another cluster characterized by the expression of markers belonging to both naïve and memory/effector cells, suggesting it could be defined by

cells in transition between these two states. Indeed, even if these cells downregulated CCR7, they expressed the naïve marker CD62L and showed the expression of adhesion molecules, such as CD103 and Integrin B7, indicating they could be an early activated subset of $CD8^+$ T cells (EA $CD8^+$_Tm) that migrated from dLNs or the blood. These cells also showed low expression of activation markers, such as CD44 and CD69, however *cd69* transcript appeared strongly upregulated, supporting the hypothesis that these cells were in a state of transition towards the activation (Fig. 2.4A).

Overall, these data allowed the identification of different and new T cell clusters based on the combination of surface markers and gene expression patterns. Interestingly, we also observed that some clusters, such as $CD8^+$ T_{RM} cells isolated from tumors, included different subclusters.

$CD8^+$ T cell subsets validation in MC38 colon cancer

To validate the presence of the new $CD8^+$ T cell subsets identified in tumors and dLNs by sc-multi-omics, we performed an immunophenotype by flow cytometry in mice injected with the MC38 colon cancer cell line. Twenty days after MC38 cells injection, both tumors and dLNs were collected. Lymphocytes were isolated, stained with fluorochrome labelled antibodies, and their phenotype was analysed by flow cytometry (Fig. 2.6A). According to the previous Ab-seq profile, we selected some surface markers, such as CD62L, CD44, PD-1, CD49d and CD103, useful in discriminating the different subpopulations and we defined a gating strategy, shown in Fig. 2.6B, in order to identify the populations of interest. We defined $CD44^+CD62L^-PD\text{-}1^{high}$ $CD103^-CD49d^-CD8^+$ cells as T_{EXH} cells. Gating on $CD8^+CD44^+CD62L^-PD\text{-}1^{low}$ cells we distinguished $CD103^-CD49d^-$ and $CD103^-CD49d^+CD8^+$ T cells, that resembled the phenotype of the T_{CYC} and the T_{RM} cells, respectively. We also validated the presence of the second subset of T_{RM} that, as opposite to the first one, was $CD62L^+CD49d^-$ (Fig. 2.6B).

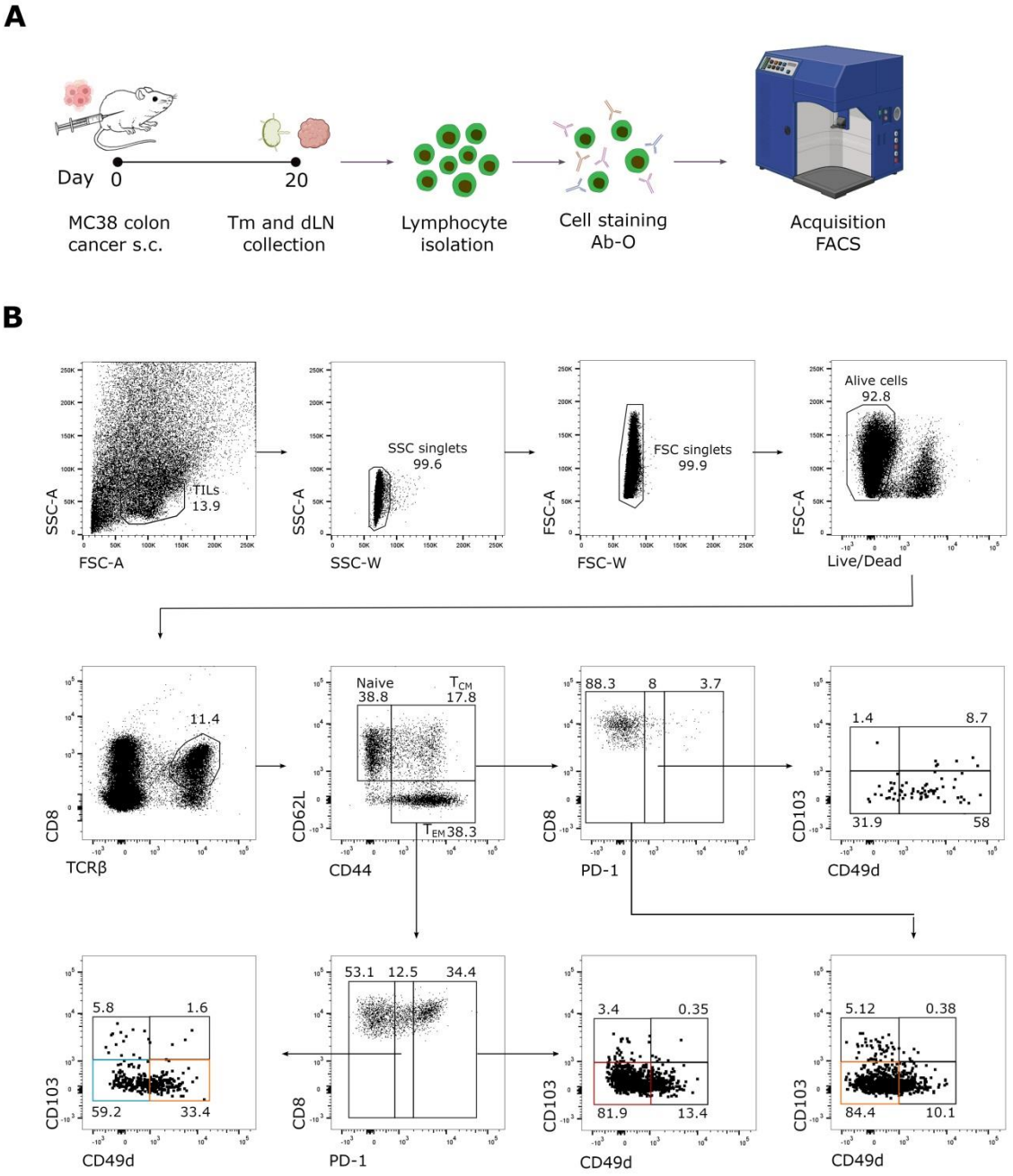

Figure 2.6. Gating strategy for *in vivo* subsets validation. (**A**) C57BL/6 mice were s.c. injected with MC38 colon carcinoma cells. After 20 days, tumors and draining lymph nodes were collected and lymphocytes isolation was performed. Cells were labelled with antibodies against specific surface markers and cells were analysed by flow cytometry. (**B**) Gating strategy ancestry: lymphocytes (FSC-A/SSC-A), SSC singlets (SSC-W/SSC-A), FSC singlets (FSC-W/FSC-A), live cells (FVS780/FSC-A), $TCR\beta^{+}CD8^{+}$ cells (BV510-TCRβ/BV786-CD8), CD44 vs CD62L (APC-R700-CD44/BV605-CD62L). PD-1 vs CD8 (SB702-PD-1/BV786-CD8) on gated $CD44^{+}CD62L^{+}$ and $CD44^{+}CD62L^{-}$ cells. CD49d vs CD103 (BV650-CD49d vs APC-CD103) on gated PD-1-, PD-1^{low} and PD-1^{high} cells. Each dot represents a single cell.

In order to study TILs heterogeneity and understand the relationships among the new identified subsets, we quantified their abundance in tumors and dLNs. First, we observed that the percentage of the $CD8^+$ T cells was higher in dLNs compared to the tumors (Fig. 2.7A). Among the $CD8^+$ T cells, naïve cells were the most abundant population in dLNs, whereas we found that around 80% of the $CD8^+$ TILs were effector T cells (Fig 2.7A). We classified T_{CM} cells in PD-1^- or PD-1^{low} cells, and T_{EM} cells in PD-1^{low} or PD-1^{high} cells. T_{CM} cells from dLNs and tumors were mostly PD-1^-, but we observed a higher frequency of PD-1^{low} T_{CM} cells among TILs compared to the cells derived from the dLNs (Fig. 2.7B). Similarly, the percentage of PD-1^{high} T_{EM} cells was significantly higher in tumors compared to dLNs, where most of T_{EM} cells were PD-1^- (Fig. 2.7C). Gating on the aforementioned populations and according to the expression of CD103 and CD49d surface markers, we distinguished: $CD49d^-CD103^-$, $CD49d^-CD103^+$, $CD49d^+CD103^-$ and $CD49d^+CD103^+$ subsets. We observed a significantly higher frequency of $CD49d^+CD103^+$ cells among PD-1^{low} T_{CM} cells isolated from tumors compared to dLN-derived lymphocytes, whereas this population was less present among PD-1^- T_{CM} cells (Fig. 2.7B). We noticed an opposite behaviour when we analysed $CD49^-CD103^-$ cells, whose frequency was lower among PD-1^{low} T_{CM} derived from tumors compared to lymphocytes isolated from lymph nodes, but they became the most prevalent population among PD-1^- T_{CM} cells. On the contrary, the majority of PD-1^{low} T_{CM} TILs were $CD49d^+CD103^-$ or $CD49d^+CD103^+$ (Fig. 2.7B). Gating on T_{EM} cells, we detected a higher frequency of $CD49d^+CD103^+$ cells among PD-1^{high} but not PD-1^{low} TILs when compared to lymph nodes (Fig. 2.7C). The most abundant population among PD-1^{low} and PD-1^{high} T_{EM} cells was $CD49d^-CD103^-$ one, both in dLNs and tumors (Fig. 2.7C). In general, we observed a similar behaviour in subsets distribution between PD-1^{low} and PD-1^{high} T_{EM} cells. Taken together these results underlie the complex relationships between different $CD8^+$ T cell subsets and their heterogeneity, and confirm the presence of different T_{RM} subsets both in dLNs and tumors.

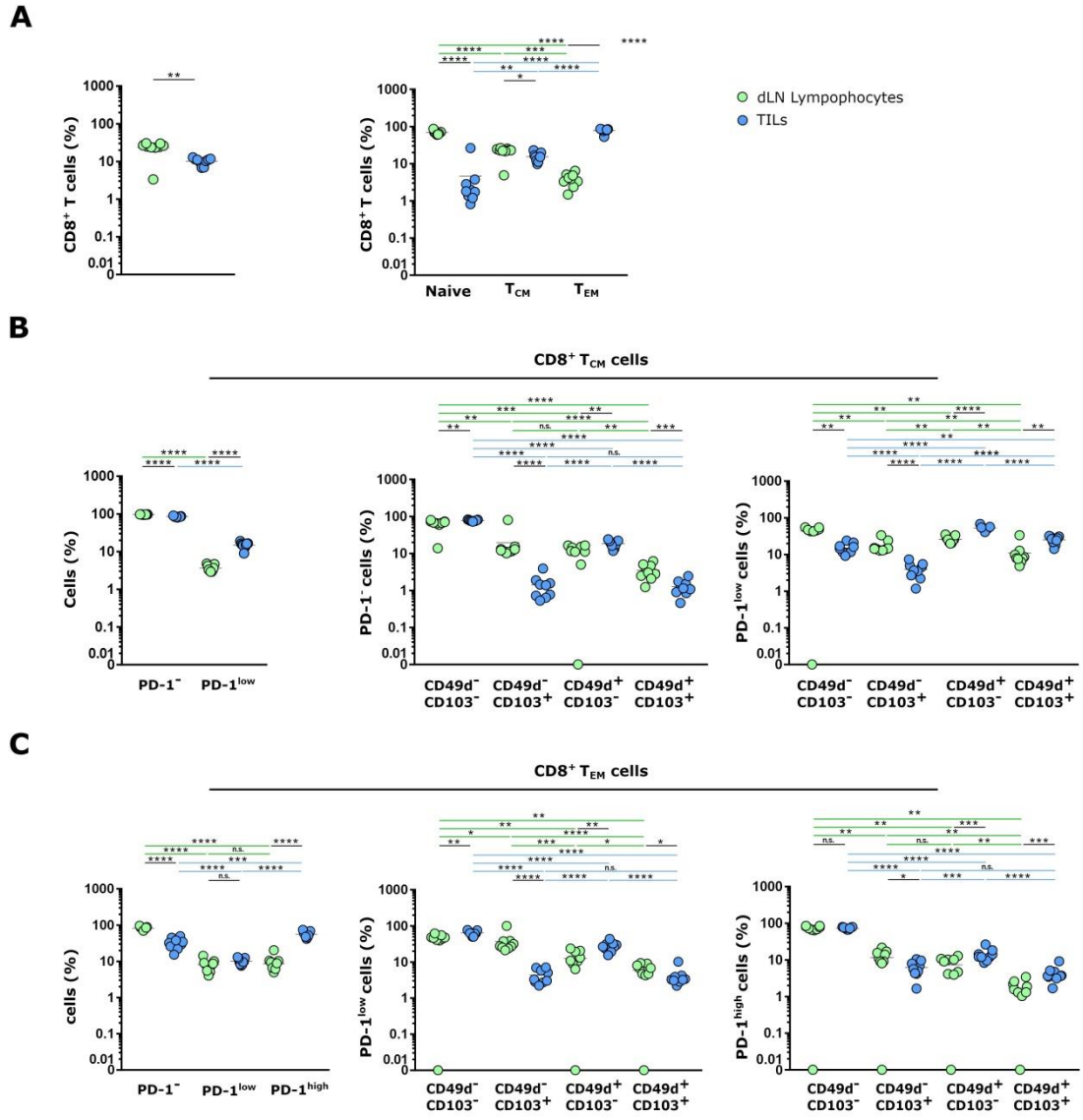

Figure 2.7. Subsets validation in MC38 tumors and dLNs. **(A-C)** Graphs showing the percentage of $CD8^+TCR\beta^+$ cells, Naïve, T_{CM} and T_{EM} $CD8^+TCR\beta^+$ cells (**A**), $CD49d^-CD103^-$, $CD49d^-CD103^+$, $CD49d^+CD103^-$ and $CD49d^+CD103^+$ cells on gated PD-1^- or PD-$1^{low}CD8^+TCR\beta^+$ T_{CM} cells (**B**) and on gated PD-1^{low} or PD-1^{high} $CD8^+TCR\beta^+$ T_{EM} cells (**C**) isolated from MC38 colon carcinoma and dLNs. Each dot represents one mouse. Statistics were calculated using Wilcoxon rank-sum test. *P < 0.05; **P < 0.01; ***P < 0.001; ****P < 0.0001; n.s.: not significant.

Subsets validation in neoepitope-specific D^b-Adpgk$^+$CD8$^+$ T cells in MC38 colon cancer

In order to investigate the different CD8$^+$ T cell responses, we decided to validate the new identified subsets also among neoantigen-specific CD8$^+$ T cells. As neoantigens can be processed and loaded on the MHC molecules of the tumor cells, they can be recognized by the TCR of CD8$^+$ T cells. Accordingly, we injected C57Bl/6 mice with the MC38 colon cancer cell line and, after the isolation of lymphocytes from tumors and dLNs, we used fluorescently labelled tetrameric MHC-peptide complexes in order to phenotypically characterize and quantify neoantigen-specific T cells by flow cytometry (Fig. 2.8A). As we injected mice with MC38 colon cancer tumor, we chose as target the Adpgk peptide from the ADP-dependent glucokinase antigen, because of its ability to elicit CD8$^+$ T cell response as previously shown (*109*). A representative dotplot of D^b-Adpgk$^+$CD8$^+$ T cells in dLN and tumor is shown in Fig. 2.8B. As expected, the percentage of D^b-Adpgk$^+$CD8$^+$ T cells was higher in tumors compared to dLNs (Fig. 2.8C).

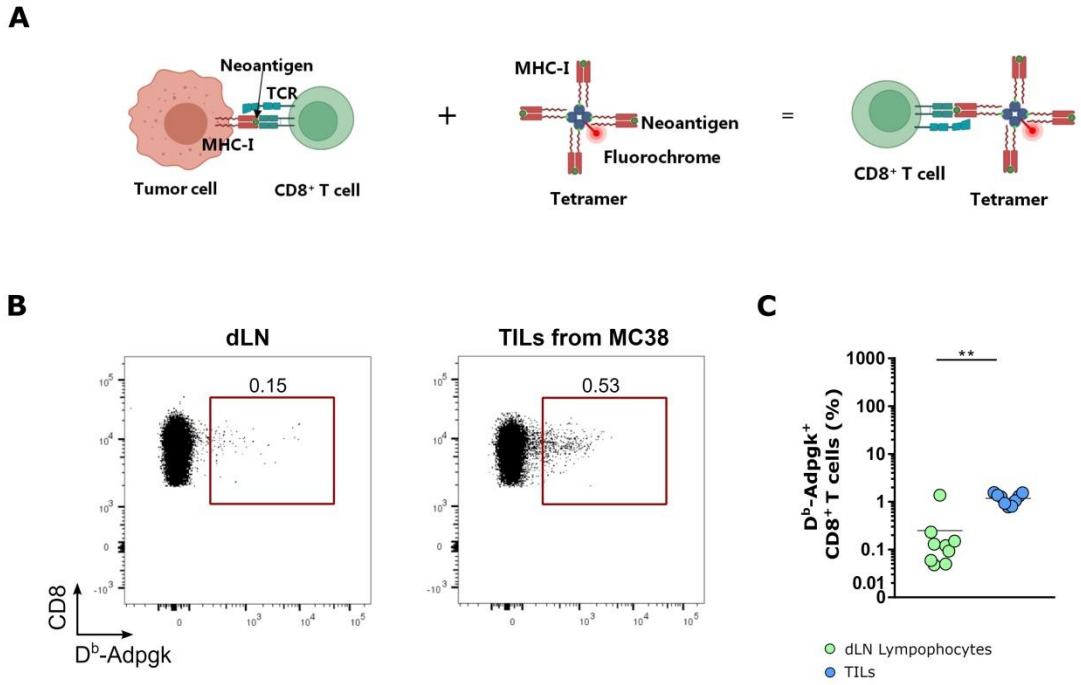

Figure 2.8. D^b-Adpgk$^+$CD8$^+$ T cell detection. (**A**) Schematic representation of antigen-specific cell detection using fluorescently labelled tetrameric MHC-peptide complex. (**B**) Representative flow cytometry dot plots of D^b-Adpgk$^+$CD8$^+$ T cells in dLN and MC38 tumor. Each dot represents a single cell. (**C**) Graphs showing the percentage of D^b-Adpgk$^+$CD8$^+$ cells in dLNs

and tumors. Each dot represents one mouse. Statistic was calculated using Wilcoxon rank-sum test. **P < 0.01.

First, we focused on the previously analysed subsets from T_{CM} and T_{EM}. No differences were observed between lymph nodes and tumors in PD-1^{-}D^{b}-Adpgk^{+}CD8^{+} T_{CM} subsets (Fig. 2.9A). On the contrary, we confirmed that, among PD-1^{low}D^{b}-Adpgk^{+}CD8^{+} T_{CM} cells isolated from tumors, the most abundant populations were CD49d^{+}CD103^{-} and CD49d^{+}CD103^{+} cells, whose frequency was significantly higher in tumors compared to dLNs. Interestingly, the latter subset was not detected among PD-1^{-}D^{b}-Adpgk^{+}CD8^{+} T_{CM} cells (Fig. 2.9A). When we analysed D^{b}-Adpgk^{+}CD8^{+} T_{EM}, we could appreciate the presence of CD49d^{+}CD103^{-} and CD49d^{+}CD103^{+} cells in both PD-1^{low} and PD-1^{high} subsets, with a significantly higher frequency among TILs compared to dLNs derived lymphocytes (Fig. 2.9B). These results confirmed the presence of our newly identified subpopulations also among neoantigen-specific CD8^{+} T cells, thus supporting the hypothesis that these subsets could play a critical role against cancer development.

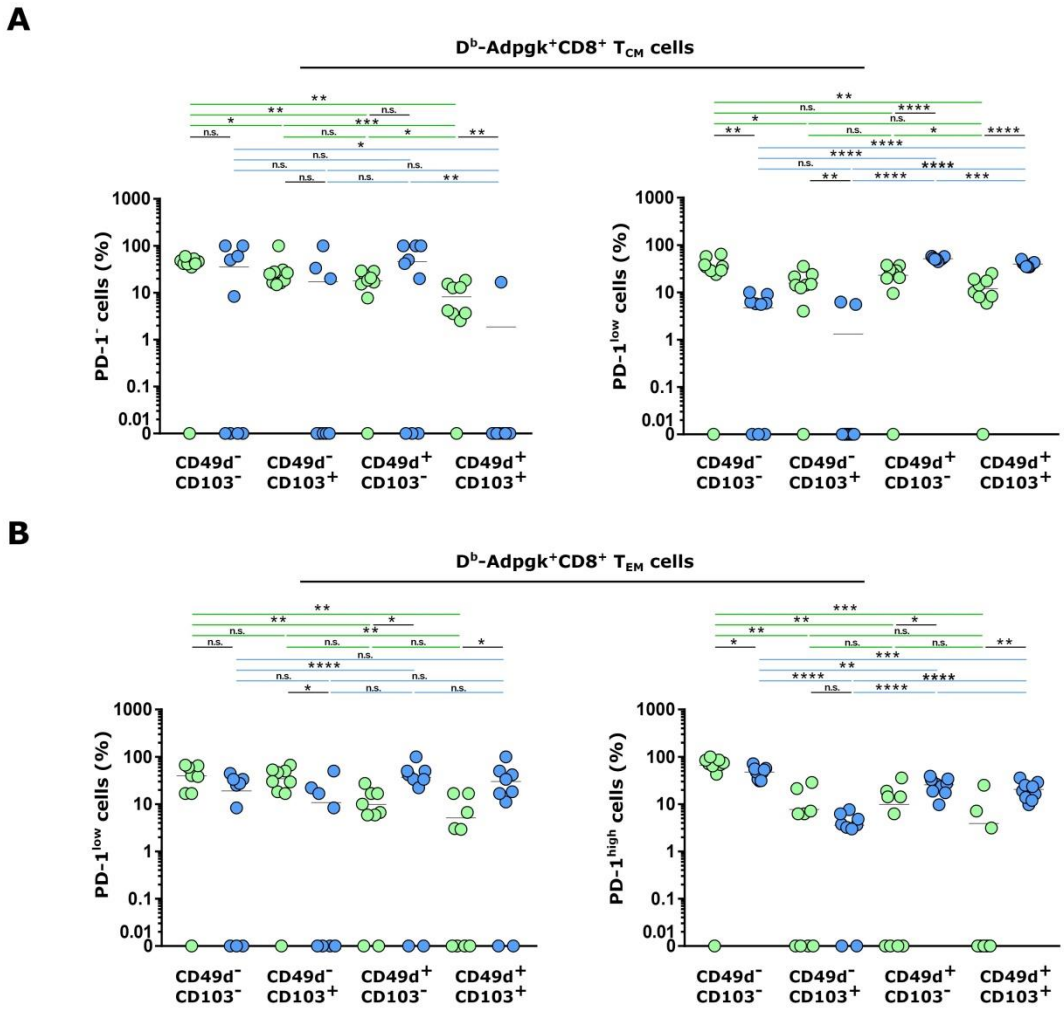

Figure 2.9. Subsets validation in D^b-Adpgk$^+$CD8$^+$ cells. (**A-B**) Graphs showing the percentage of CD49d$^-$CD103$^-$, CD49d$^-$CD103$^+$, CD49d$^+$CD103$^-$ and CD49d$^+$CD103$^+$ cells on gated PD-1$^-$ or PD-1^{low} D^b-Adpgk$^+$CD8$^+$ T_{CM} cells (**A**) and on gated PD-1^{low} or PD-1^{high} D^b-Adpgk$^+$CD8$^+$ T_{EM} cells (**B**) isolated from MC38 colon carcinoma and dLNs. Each dot represents one mouse. Statistics were calculated using Wilcoxon rank-sum test. *P < 0.05; **P < 0.01; ***P < 0.001; ****P < 0.0001; n.s.: not significant.

CD8$^+$ T cell subsets validation in MC38.OVA colon cancer

To study the immune responses elicited by a stronger neoepitope as compared to Adpgk, C57BL/6 mice were s.c. injected with MC38 colon carcinoma expressing ovalbumin peptide SIINFEKL (MC38.OVA). Tumor growth was measured every three days, until day twenty post-injection, when mice were sacrificed (Fig. 2.10).

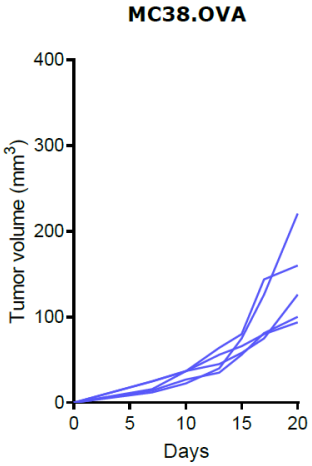

Figure 2.10. MC38.OVA colon carcinoma growth. Mice were s.c. injected with MC38.OVA tumor cell line and tumor size was measured every three days with a caliper.

After isolation from tumors and dLNs, lymphocytes were stained with fluorochrome labelled antibodies and analysed by flow cytometry. When we analysed the total $CD8^+$ cells, the most abundant subset among PD-1^- T_{CM} cells was $CD103^-$, whereas $CD103^+$ cell frequency was quite low. On the contrary, when we focused on the PD-1^{low} T_{CM} cells, we observed the presence of $CD103^+$ cells, even if their frequency was not different in tumors compared to dLNs (Fig. 2.11A). Among T_{EM} cells, we observed a similar distribution of PD-1^{low} and PD-1^{high} subsets, with higher frequencies of $CD103^-$ subsets, both in dLNs and tumors (Fig. 2.11B).

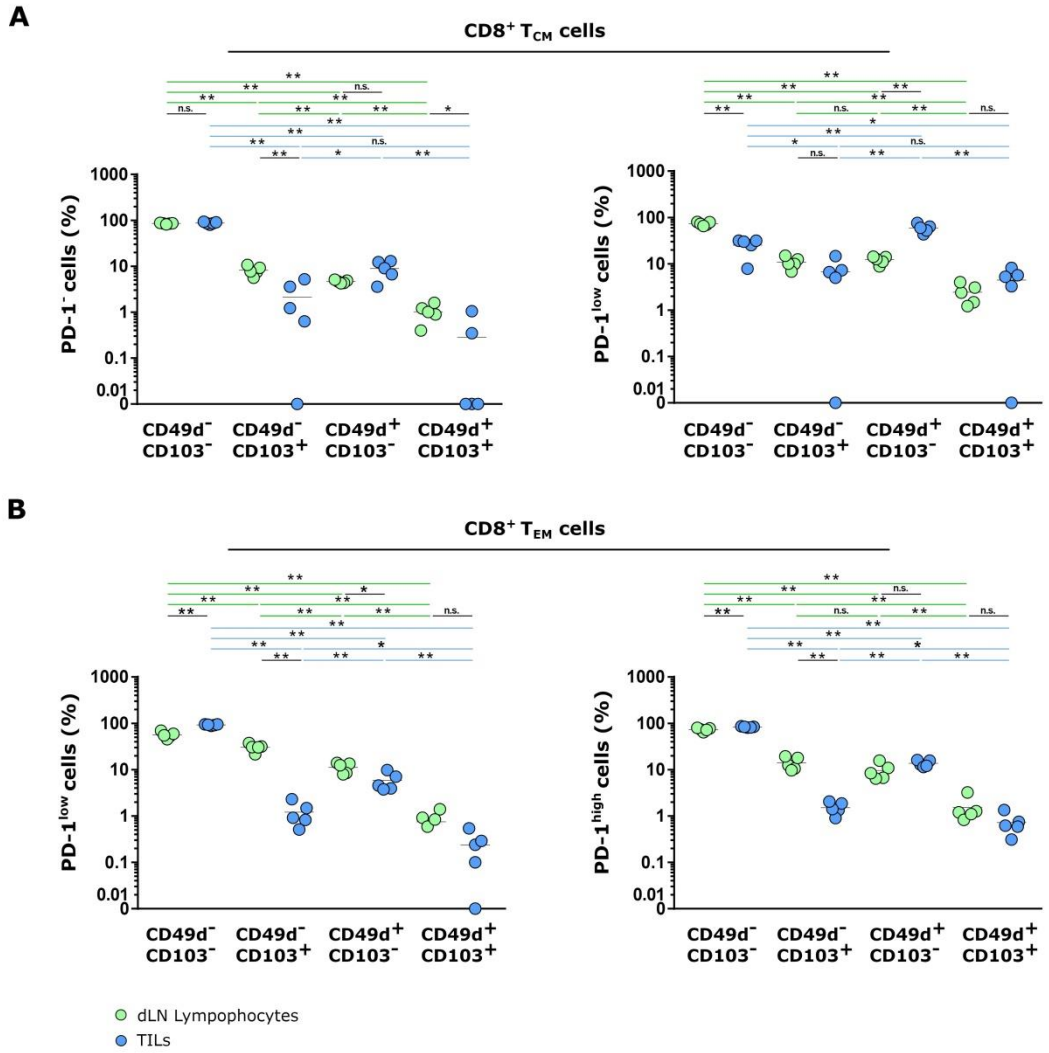

Figure 2.11. Subsets validation in MC38.OVA tumors and dLNs. (**A-B**) Graphs showing the percentage of $CD49d^{-}CD103^{-}$, $CD49d^{-}CD103^{+}$, $CD49d^{+}CD103^{-}$ and $CD49d^{+}CD103^{+}$ cells on gated PD-1^{-} or PD-1^{low} $CD8^{+}$ T_{CM} (**A**) and on gated PD-1^{low} or PD-1^{high} $CD8^{+}$ T_{EM} (**B**) cells isolated from MC38.OVA colon carcinoma and dLNs. Each dot represents one mouse. Statistics were calculated using Wilcoxon rank-sum test. *P < 0.05; **P < 0.01; n.s.: not significant.

Subsets validation in K^{b}-SIINFEKL$^{+}CD8^{+}$ T cells from MC38.OVA colon cancer

After the analysis of total $CD8^{+}$ T cells, we focused on neoepitope-specific K^{b}-SIINFEKL$^{+}CD8^{+}$ T cells. Representative dotplots of K^{b}-SIINFEKL$^{+}CD8^{+}$ T cells in dLN and tumor are shown in Fig. 2.12A. In accordance with the results of D^{b}-Adpgk$^{+}CD8^{+}$ T cells, also the percentage of K^{b}-SIINFEKL$^{+}CD8^{+}$ T cells was significantly higher in tumors compared to dLNs (Fig. 2.12B). According to what we observed on total $CD8^{+}$ T_{CM} cells, PD-$1^{-}K^{b}$-SIINFEKL$^{+}CD8^{+}$ T_{CM} cells isolated from tumors expressed low level of CD103 T_{RM} marker, whereas in PD-$1^{low}K^{b}$-

SIINFEKL^{+}CD8^{+} T_{CM} from tumors we could detect higher level of CD103 in 3/5 mice (Fig. 2.12C). When we analyzed K^{b}-SIINFEKL^{+}CD8^{+} T_{EM} cells, the subset distribution and frequencies mirrored what we previously observed with total CD8^{+} cells, except for the CD49d^{+}CD103^{+} K^{b}-SIINFEKL^{+}CD8^{+} T_{EM}, whose frequency was very low among PD-1^{low} cells but increased in PD-1^{high} cells (Fig. 2.12D).

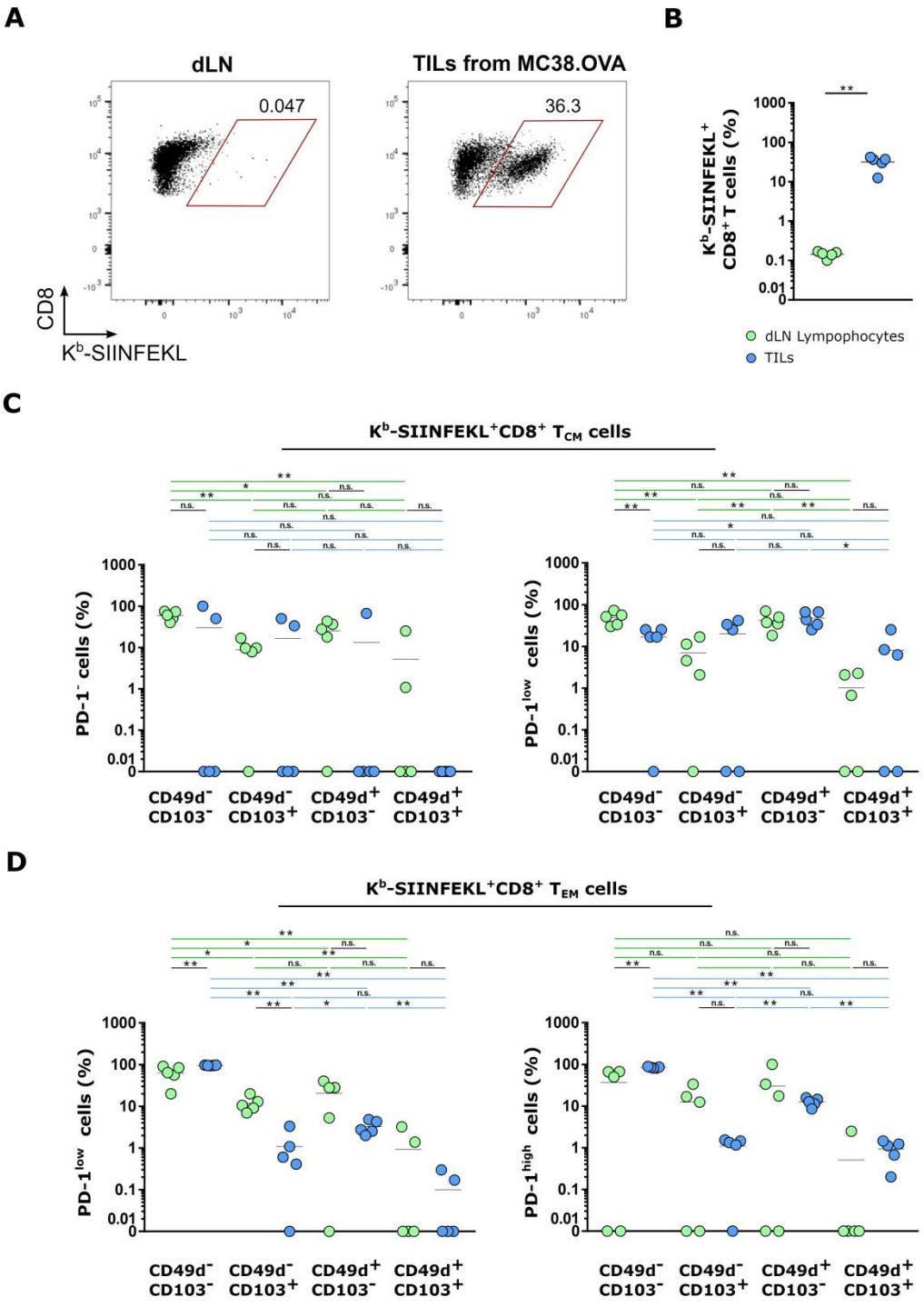

Figure 2.12. Subsets validation in K^b-SIINFEKL$^+$CD8$^+$ T cells from MC38.OVA tumors and dLNs. (**A**) Representative flow cytometry dot plots of K^b-SIINFEKL$^+$CD8$^+$ cells in dLN and MC38.OVA tumor. Each dot represents one single cell. (**B-D**) Graphs showing the percentage of K^b-SIINFEKL$^+$CD8$^+$ cells (**B**), CD49d$^-$CD103$^-$, CD49d$^-$CD103$^+$, CD49d$^+$CD103$^-$ and CD49d$^+$CD103$^+$ cells on gated PD-1$^-$ or PD-1^{low} K^b-SIINFEKL$^+$CD8$^+$ T_{CM} (**C**) and on gated PD-1^{low} or PD-1^{high} K^b-SIINFEKL$^+$CD8$^+$ T_{EM} (**D**) cells isolated from MC38.OVA colon carcinoma and dLNs. Each dot represents one mouse. Statistics were calculated using Wilcoxon rank-sum test. *P < 0.05; **P < 0.01; n.s.: not significant.

Overall, these results suggest that CD8$^+$ T cell differentiation and subsets frequency could be related to the different TCR affinity for each neoepitope. Because Adpgk is a self-neoantigen, it has lower affinity for its TCR when compared to SIINFEKL epitope from chicken ovalbumin that is a strong non-self-antigen (*110*). According to this, our results suggest that when the immune system is activated by a neoantigen such as Adpgk, specific immune cell subsets could upregulate the expression of CD49d and CD103 and differentiate in T_{RM} subsets, whereas when the neoepitope has higher affinity and expression level, the frequency of these subsets is reduced.

CD8$^+$ T cell subsets distribution in poorly immunogenic tumor

The effectiveness of cancer immunotherapies often relies on the immunogenicity of the tumor. Immunogenicity is defined as the ability of a molecule or substance to provoke an immune response. Because MC38 colon carcinoma has a high mutational burden, it is considered a highly immunogenic tumor. Anyway, the most challenging tumors are those that do not respond to immunotherapies because of their ability to escape the immune system. So, we wondered if different tumor immunogenicity was also associated to different distribution and frequencies of our newly identified subsets. To answer this question, we chose the B16F10.OVA melanoma, that belong to the group of the so called “cold tumors” as it shows very low or absent immune infiltrates.

We injected C57BL/6 mice with B16F10.OVA cells and, in line with melanoma aggressiveness, we observed faster tumor growth and greater tumor volume when mice were injected with B16F10.OVA melanoma compared to MC38.OVA colon carcinoma (Fig. 2.10 and 2.13).

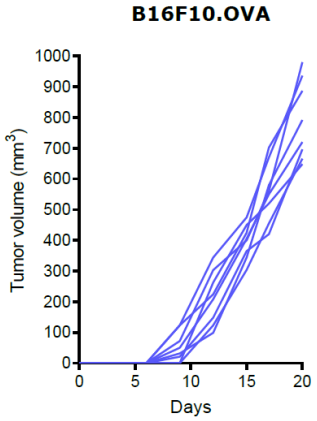

Figure 2.13. B16F10.OVA melanoma growth. Mice were s.c. injected with B16F10.OVA tumor cell line and tumor size was measured every three days with a caliper.

After twenty days from injection, we isolated TILs and lymphocytes from dLNs and analysed their phenotype by flow cytometry. On total $CD8^+$ T cells we observed that the most abundant subsets in both PD-1^- and PD-1^{low} T_{CM} cells were $CD49d^-CD103^-$ and $CD49d^+CD103^-$ cells, with significantly higher frequency of $CD49d^+CD103^-$ cells in tumors compared to dLNs. There was no difference in the abundancy of $CD103^+CD49d^+$ cells between the two compartments, whereas we observed a lower frequency of $CD49d^-CD103^+$ cells in TILs respect to the dLNs derived cells. Also, $CD8^+$ T_{EM} cells showed a lower frequency of $CD103^+$ TILs subsets both in PD-1^{low} and PD-1^{high} subpopulations, whereas $CD103^-$ cells represented the most dominant subset (Fig. 2.14A-B).

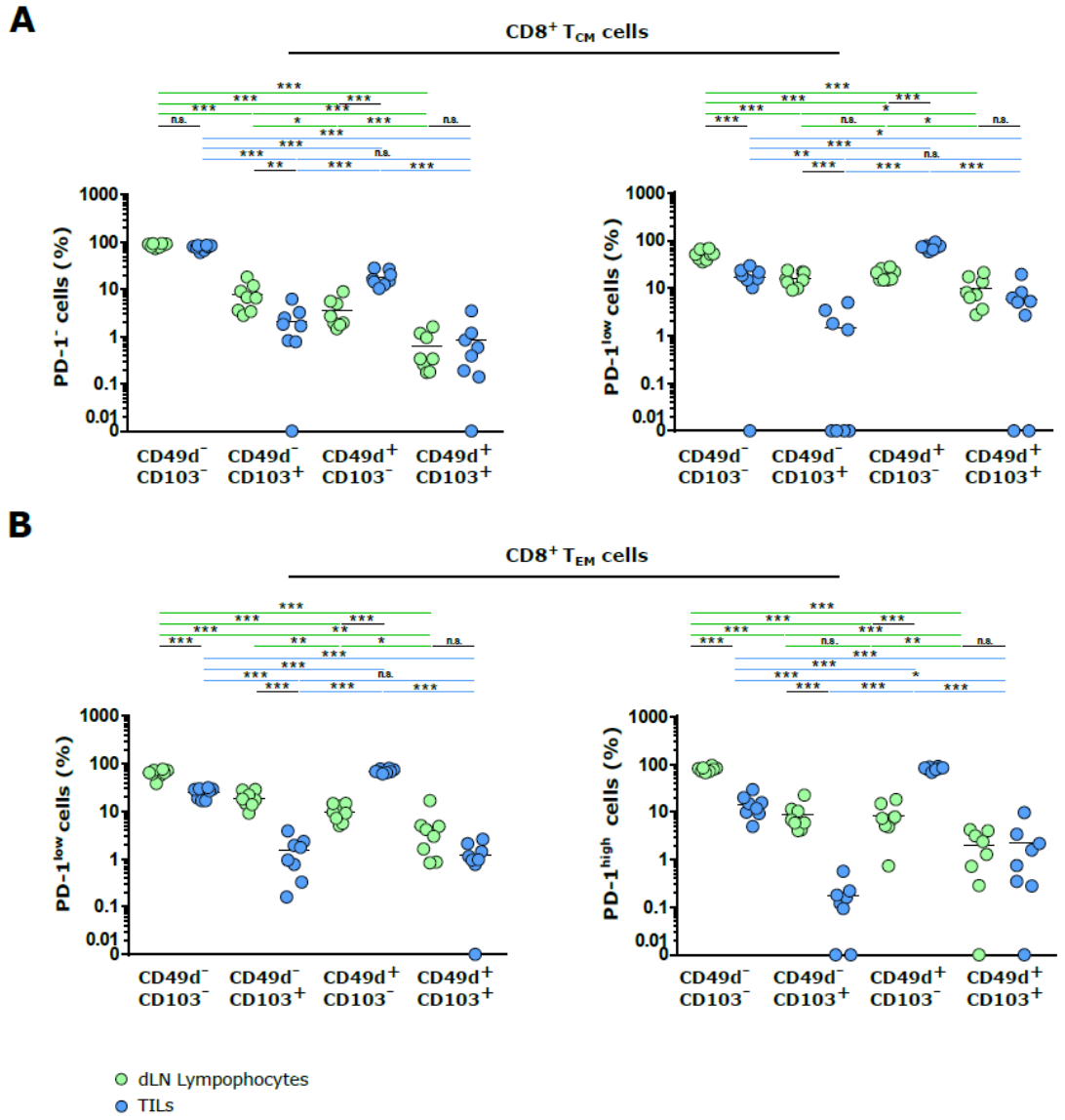

Figure 2.14 Subsets validation in B16F10.OVA tumors and dLNs. (**A-B**) Graphs showing the percentage of $CD49d^{-}CD103^{-}$, $CD49d^{-}CD103^{+}$, $CD49d^{+}CD103^{-}$ and $CD49d^{+}CD103^{+}$ cells on gated PD-1^{-} or PD-$1^{low}CD8^{+}T_{CM}$ cells (**A**) and on gated PD-1^{low} or PD-1^{high} $CD8^{+}$ T_{EM} cells (**B**) isolated from B16F10.OVA melanoma and dLNs. Each dot represents one mouse. Statistics were calculated using Wilcoxon rank-sum test. *P < 0.05; **P < 0.01; ***P < 0.001; n.s.: not significant.

Subsets validation with neoepitope-specific K^{b}-SIINFEKL$^{+}CD8^{+}$ T cells from B16F10.OVA melanoma

After the analysis of total $CD8^{+}$ T cells, we analysed neoepitope-specific $CD8^{+}$ T cells. Representative dotplots of K^{b}-SIINFEKL$^{+}CD8^{+}$ cells isolated from dLN and tumor are shown in Fig. 2.15A. Quantification of K^{b}-SIINFEKL$^{+}CD8^{+}$ T cells showed that their

frequency was higher in tumors compared to dLNs (Fig. 2.15B). When we focused on our subsets of interest, we observed that CD103 was downregulated in PD-1^{-} T_{CM} and PD-1^{low} T_{EM} K^b-SIINFEKL^{+}CD8^{+} T cells isolated from tumors, indeed we could not detect CD49d^{+}CD103^{+} cells (Fig. 2.15 C-D). By contrast, we could distinguish CD49d^{+}CD103^{+} cells on PD-1^{low} T_{CM} and PD-1^{high} T_{EM} K^b-SIINFEKL^{+}CD8^{+} T cells from tumors (Fig. 2.15C-D). In accordance with the results with total CD8^{+} T cells, CD49d^{-}CD103^{-} and CD49d^{+}CD103^{-} subsets were the most abundant among K^b-SIINFEKL^{+}CD8^{+} TILs (Fig. 2.15C-D).

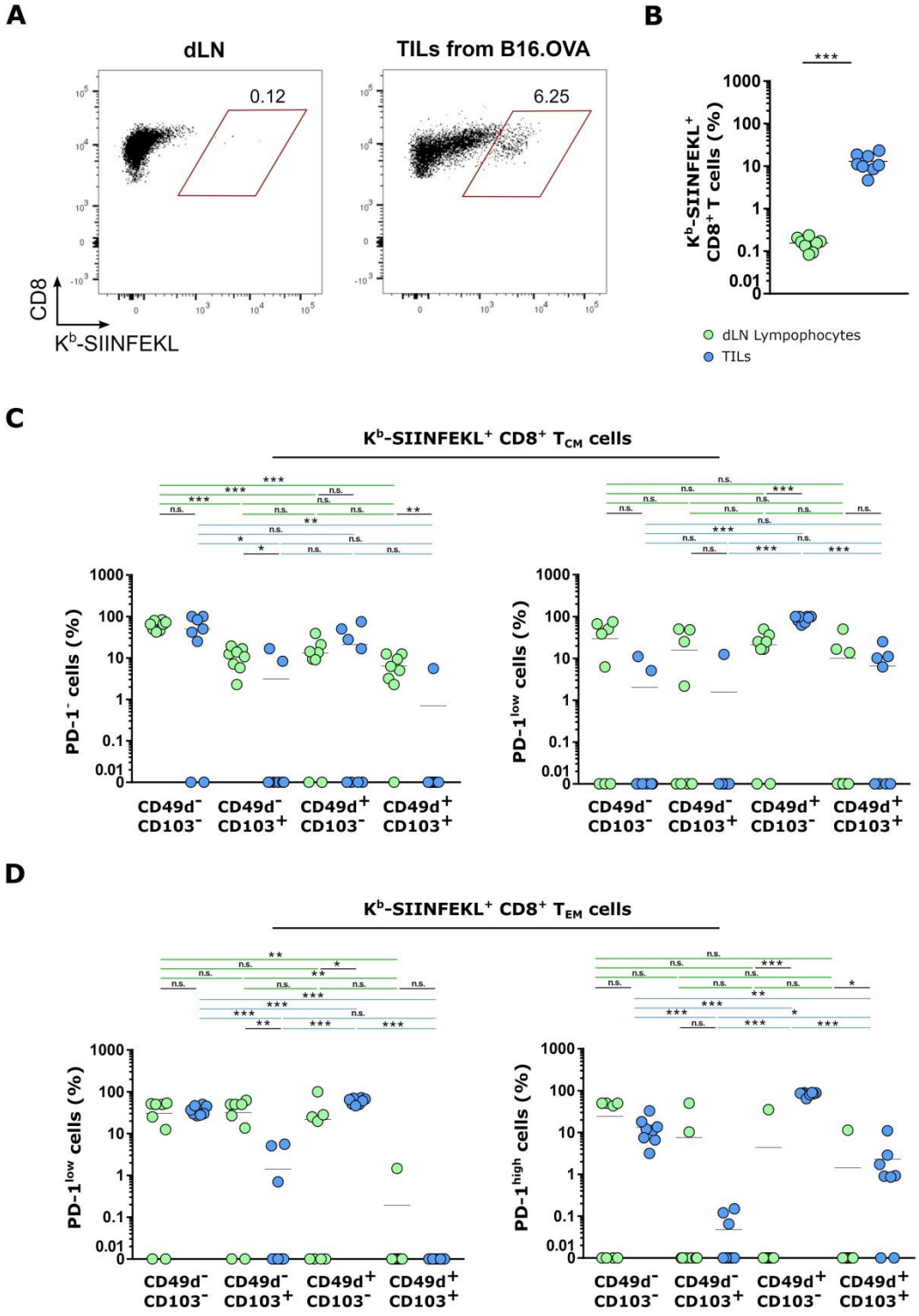

Figure 2.15. Subsets validation in K^b-SIINFEKL$^+$CD8$^+$ T cells from B16F10.OVA tumors and dLNs. (**A**) Representative flow cytometry dot plots of K^b-SIINFEKL$^+$ CD8$^+$ T cells in dLN and tumor. Each dot represents one single cell. (**B-D**) Graphs showing the percentage of K^b-SIINFEKL$^+$CD8$^+$ T cells (**B**), CD49d$^-$CD103$^-$, CD49d$^-$CD103$^+$, CD49d$^+$CD103$^-$ and CD49d$^+$CD103$^+$ cells on gated PD-1$^-$ or PD-1^{low} K^b-SIINFEKL$^+$ CD8$^+$ T_{CM} cells (**C**) and on gated PD-1^{low} or PD-1^{high} K^b-SIINFEKL$^+$CD8$^+$ T_{EM} cells (**D**) isolated from B16F10.OVA

melanoma and dLNs. Each dot represents one mouse. Statistics were calculated using Wilcoxon rank-sum test. *P < 0.05; **P < 0.01; n.s.: not significant.

Overall, we observed a higher frequency of $CD49d^{+}CD103^{+}$ cells in both $CD8^{+}$ T_{CM} and T_{EM} cells isolated from MC38 tumor compared to MC38.OVA colon carcinoma and this difference was statistically significant (Fig. 2.16A). The same result was confirmed among antigen-specific $CD8^{+}$ T cells, except in the subset of $PD\text{-}1^{-}CD8^{+}$ T_{CM} cells (Fig. 2.16B). Conversely, $CD49d^{-}CD103^{-}PD\text{-}1^{low}$ and $CD49d^{-}CD103^{-}PD\text{-}1^{high}$ T_{EM} cells were significantly lower in MC38 compared to MC38.OVA tumors, in both total $CD8^{+}$ and antigen-specific $CD8^{+}$ T cells (Fig. 2.16 A-B). In MC38 we also observed a higher frequency of $CD49d^{-}CD103^{+}PD\text{-}1^{low}$ and $CD49d^{-}CD103^{+}PD\text{-}1^{high}$ $CD8^{+}$ T_{EM} cells (Fig. 2.16A). Taken together these data sustain the hypothesis that a stronger antigen can elicit a different immune response characterized by the differentiation of certain subpopulations compared to others.

A distinct immune subset distribution was also evident when we compared highly and poorly immunogenic tumors. The main differences between the MC38.OVA colon cancer and the B16F10.OVA melanoma $CD8^{+}$ T cells were among T_{EM} cells. Indeed, compared to MC38.OVA, TILs isolated from B16F10.OVA tumors showed lower percentage of $CD49d^{-}CD103^{-}PD\text{-}1^{low}$ and $CD49d^{-}CD103^{-}PD\text{-}1^{high}$ $CD8^{+}$ T_{EM} subsets, that, according to our initial analysis, we identified as T_{CYC} and T_{EXH} subpopulations, respectively (Fig. 2.16A). Moreover, $CD49d^{-}CD103^{+}PD\text{-}1^{high}CD8^{+}$ T_{EM} cell frequency was lower in TILs isolated from poorly immunogenic tumors compared to highly ones (Fig. 2.16A). These results were confirmed among $K^{b}\text{-}SIINFEKL^{+}CD8^{+}$ T cells (Fig. 2.16B). By contrast, we observed an increase of $CD49d^{+}CD103^{-}PD\text{-}1^{low}$ and $CD49d^{+}CD103^{-}PD\text{-}1^{high}$ T_{EM} cells in both total $CD8^{+}$ and $K^{b}\text{-}SIINFEK^{+}CD8^{+}$ cells isolated from B16F10.OVA compared to MC38.OVA tumors (Fig. 2.16A-B). These data were confirmed when we analysed the antigen-specific $CD8^{+}$ T cells (Fig. 2.16B). Taken together these results highlight that tumor immunogenicity can strongly impact T cell differentiation towards subpopulations with distinct immunophenotypes and different efficacy in fighting cancer progression.

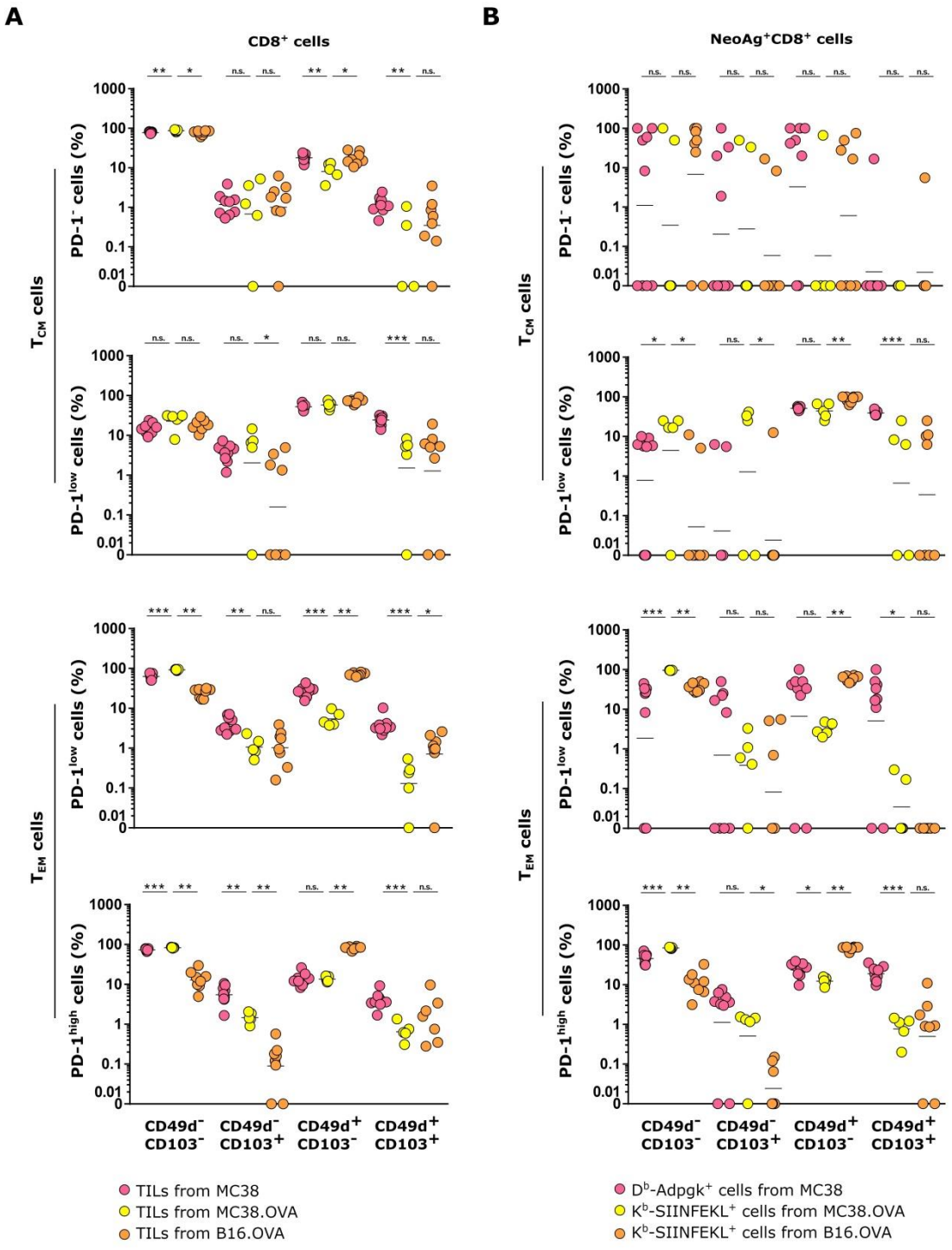

Figure 2.16. Comparison among TILs isolated from highly and poorly immunogenic tumors. (**A**) Graphs showing the percentage of $CD49d^{-}CD103^{-}$, $CD49d^{-}CD103^{+}$, $CD49d^{+}CD103^{-}$ and $CD49d^{+}CD103^{+}$ cells on gated PD-1^{-} or PD-1^{+}CD8 T_{CM} and on gated PD-1^{low} or PD-1^{high} $CD8^{+}$ T_{EM} cells isolated from MC38, MC38.OVA and B16F10.OVA tumors. (**B**) Graphs showing the percentage of $CD49d^{-}CD103^{-}$, $CD49d^{-}CD103^{+}$, $CD49d^{+}CD103^{-}$ and $CD49d^{+}CD103^{+}$ cells on gated antigen-specific PD-1^{-} or PD-$1^{+}CD8^{+}$ T_{CM} and on gated antigen-specific PD-1^{low} or PD-1^{high} $CD8^{+}$ T_{EM} cells isolated from MC38, MC38.OVA and B16F10.OVA tumors. Each dot represents one mouse. Statistics were calculated using

Wilcoxon rank-sum test. *P < 0.05; **P < 0.01; ***P < 0.001; ****P < 0.0001; n.s.: not significant.

$CD8^+$ T cell subsets distribution in KP lung cancer

We relied on the Kras-Lox-STOP-Lox-G12D p53 flox/flox (KP^{Ctr}) lung cancer model to confirm the results that we obtained comparing poorly and highly immunogenic tumors. This tumor upregulates the mutated oncogene Kras, it lacks the tumor suppressor Trp53 and, as it expresses few neoantigens, it elicits poor T cell responses and it is considered poorly immunogenic (López Rodríguez et al., Nat. Commun, manuscript in press). On the contrary, the hypermutated variant of this model, named KP^{Neo}, generated by the deletion of a core protein in the DNA repair machinery (Mlh1), produces a number of neoantigens and it is highly immunogenic (López Rodríguez et al., Nat. Commun, manuscript in press). We injected mice s.c. with KP^{Ctr} and KP^{Neo} cancer cells. Because of their immunogenicity and aggressiveness, KP^{Ctr} tumor grew faster compared to KP^{Neo} one (Fig. 2.17).

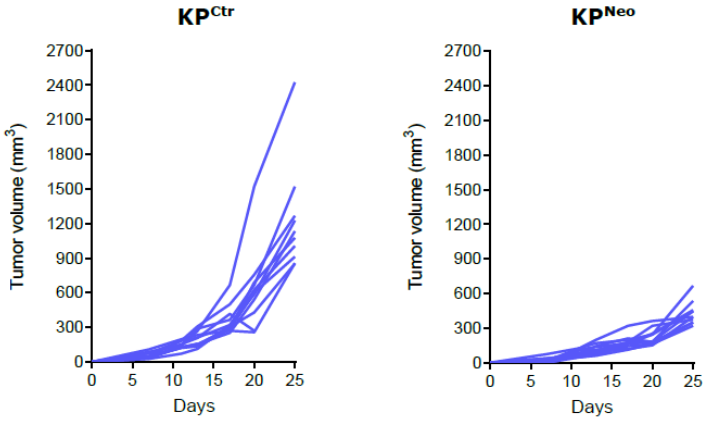

Figure 2.17. KP tumor growth. Mice were s.c. injected with KP^{Ctr} or KP^{Neo} tumor cell line and tumor size was measured every three days with a caliper.

After twenty-six days from injection, lymphocytes were isolated from tumors and dLNs, and analysed by flow cytometry. Focusing on our specific subsets of interest, we didn't detect significant differences in the frequencies of the lymphocyte's subpopulations isolated from KP^{Ctr} tumors and dLNs. We only observed that $CD49d^-CD103^-$ cells represented the most abundant subset among $PD\text{-}1^-CD8^+$ T_{CM} cells (Fig. 2.18). Moreover, in KP^{Neo} tumors and dLNs we observed the same results (Fig. 2.18). As seen in TILs isolated from MC38 tumor, we detected a very low frequency of

$CD49d^+CD103^+$ cells among PD-1^- $CD8^+$ T_{CM} from KP^{Neo} tumor, which conversely incremented on gated PD-$1^{low}CD8^+$ T_{CM}, even if we could not appreciate significant differences when compared to the other subsets from the same gate (Fig. 2.18).

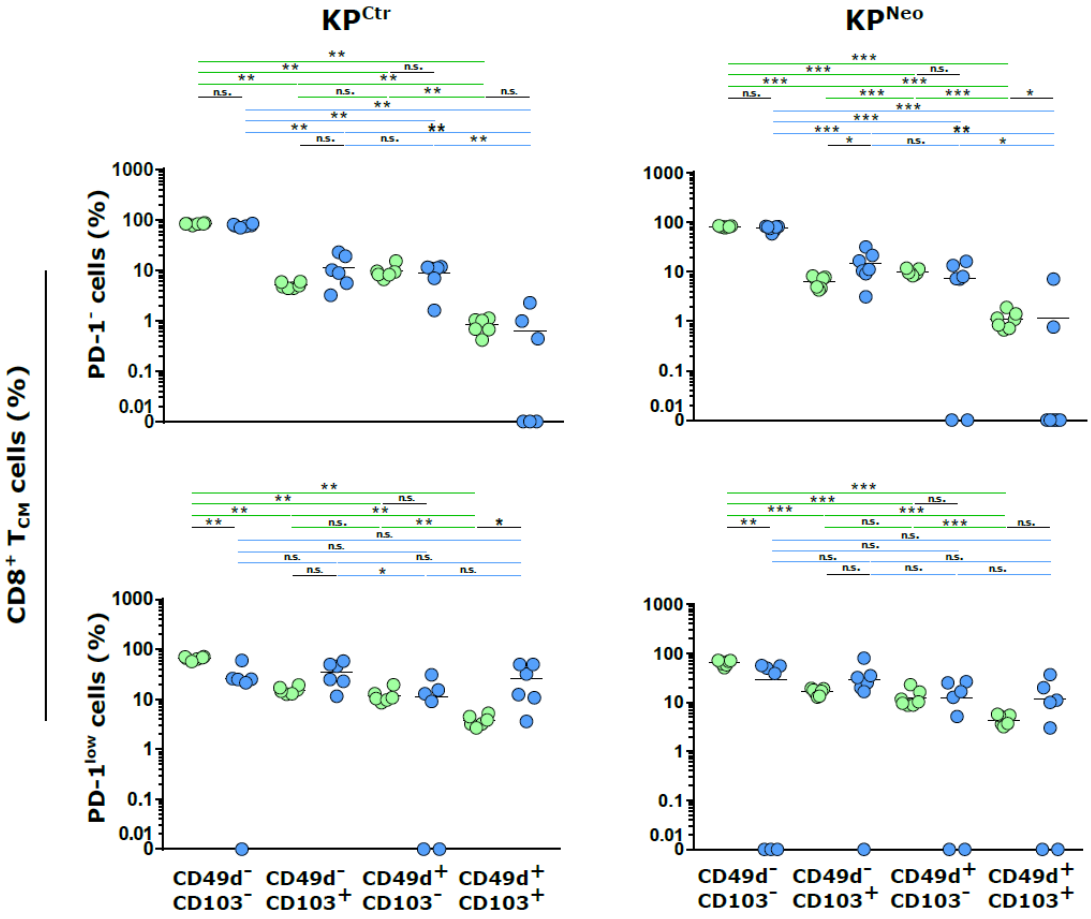

Figure 2.18. Subsets validation in $CD8^+$ T_{CM} cells from KP tumors and dLNs. Graphs showing the percentage of $CD49d^-CD103^-$, $CD49d^-CD103^+$, $CD49d^+CD103^-$ and $CD49d^+CD103^+$ cells on gated PD-1^- or PD-1^{low} $CD8^+$ T_{CM} cells isolated from KP^{Ctr} and KP^{Neo} lung tumors and dLNs. Each dot represents one mouse. Statistics were calculated using Wilcoxon rank-sum test. *P < 0.05; **P < 0.01; ***P < 0.001; n.s.: not significant.

Among $CD8^+$ T_{EM} cells, we noticed a higher frequency of $CD49d^-CD103^-$ and $CD49d^-CD103^+$ subsets on gated PD-1^{high} cells from KP^{Neo} tumors when compared to dLNs. Moreover, the abundancy of these populations in the tumors was statistically higher when compared to $CD49d^+CD103^-$ and $CD49d^+CD103^+$ subsets both in PD-1^{low} and PD-1^{high} $CD8^+$ TILs (Fig. 2.19).

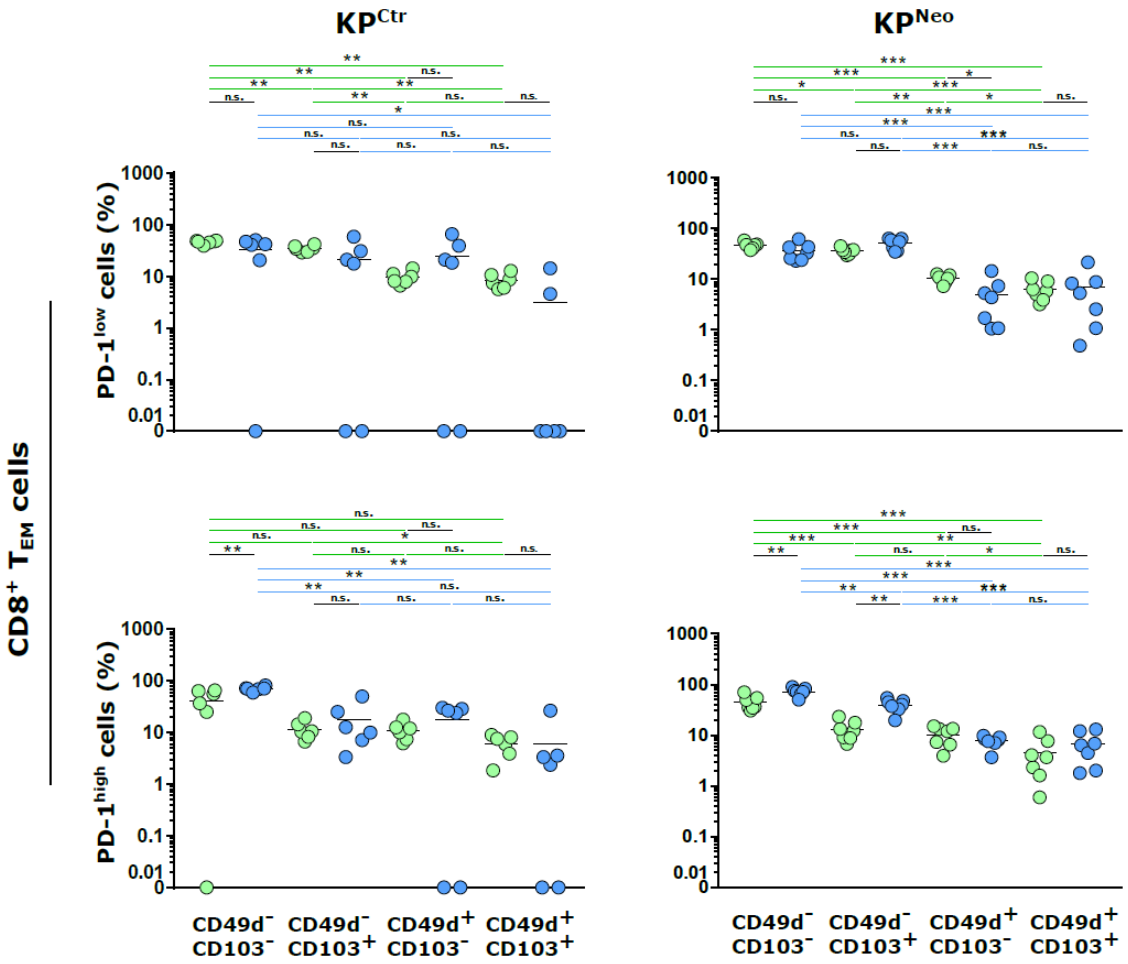

Figure 2.19. Subsets validation in CD8$^+$ T$_{EM}$ cells from KP tumors and dLNs. Graphs showing the percentage of CD49d$^-$CD103$^-$, CD49d$^-$CD103$^+$, CD49d$^+$CD103$^-$ and CD49d$^+$CD103$^+$ cells on gated PD-1^{low} or PD-1^{high} CD8$^+$ T$_{EM}$ cells isolated from KP^{Ctr} and KP^{Neo} lung tumors and dLNs. Each dot represents one mouse. Statistics were calculated using Wilcoxon rank-sum test. *P < 0.05; **P < 0.01; ***P < 0.001; n.s.: not significant.

Then, we analysed and quantified the neoepitope-specific CD8$^+$ T cells in KP tumors and dLNs. To do this, we relied on some bioinformatically predicted putative neoepitopes shared by KP^{Ctr} and KP^{Neo} (López Rodríguez et al., Nat. Commun, manuscript in press), which were analyzed to establish their expression levels (TPM) and predicted MHC-I affinities (IC_{50}) (Table 1).

List of neoepitopes

Neo-Ag	PREDICTED IC_{50}	EXPRESSION (TPM)
Ne1	1162,21	35,9666667
Ne2	262,32	6,17
Ne3	1249,32	13,6833333
Ne4	468,28	325,745
Ne5	1014,62	25,2983333
Ne6	1521,89	35,9666667
Ne7	146,75	3,83166667
Ne8	115,12	15,9316667
Ne9	32,91	2,41
Ne10	637,98	7,90166667
Ne11	1466,52	10,67
Ne12	47,63	30,095
Ne13	125,28	36,85
Ne14	23,17	13,4216667
Ne15	64,67	38,0466667
Ne16	1466,96	25,1483333
Ne17	185,41	5,84336508
Ne18	167,72	16,5975
Ne19	6,2	78,6466667
Ne20	21,77	78,6466667
Ne21	23	78,6466667
Ne22	133,39	78,6466667

Table 1. List of neoepitopes. Putative neoepitopes identified in KP^{Ctr} and KP^{Neo} cells are listed based on their predicted affinity for MHC-I (IC_{50}) and their expression levels (TPM) (López Rodríguez et al., Nat. Commun, manuscript in press).

We selected two neoepitopes, number 4 (Ne4) and 22 (Ne22), and we quantified the neoepitope-specific $CD8^+$ T cells in KP^{Ctr} and KP^{Neo}. Ne4 had low affinity for its MHC-I but high expression level (TPM), conversely Ne22 had higher affinity and lower expression level.

When we analysed D^b-$Ne4^+$ and D^b-$Ne22^+CD8^+$ T cells, we observed only a higher percentage of D^b-$Ne4^+CD8^+$ T cells in KP^{Neo} tumors compared to dLNs (Fig. 2.20). Although we didn't notice any other significant difference in the frequency of D^b-$Ne4^+$ and D^b-$Ne22^+CD8^+$ T cells in KP^{Ctr} or KP^{Neo} tumors compared to dLNs, we decided to further analyse D^b-$Ne22^+CD8^+$ T cells as we could detect them both in KP^{Ctr} and KP^{Neo} tumors and dLNs.

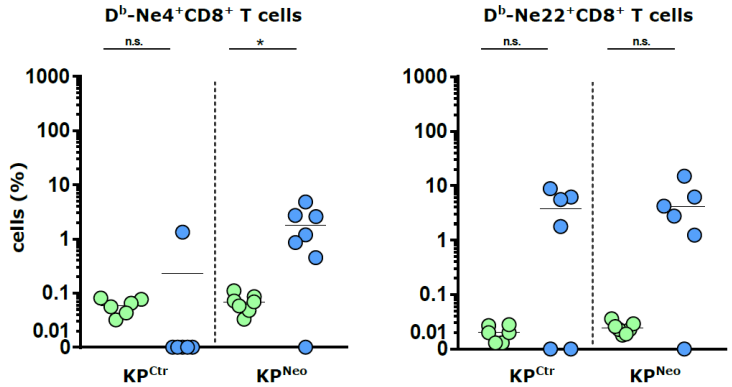

Figure 2.20. Neoantigen-specific $CD8^+$ T cells in KP tumors and dLNs. Graphs showing the percentage of D^b-$Ne4^+CD8^+$ and D^b-$Ne22^+CD8^+$ T cells in KP^{Ctr} or KP^{Neo} tumors and lymph nodes. Each dot represents one single mouse. Statistics were calculated using Wilcoxon rank-sum test. *P < 0.05; n.s.: not significant.

In KP^{Ctr} tumor bearing mice, we could detect D^b-$Ne22^+CD8^+$ T cells among $CD49d^-$ $CD103^-$ and $CD49d^+CD103^-PD\text{-}1^-$ T_{CM} cells isolated from dLNs and among $PD\text{-}1^{low}$ T_{CM} cells from both tumors (3/6 or 2/6 mice) and dLNs, but we could not appreciate any significant difference between the different subpopulations. In mice injected with KP^{Neo} tumor, we found D^b-$Ne22^+CD8^+$ T_{CM} cells only in dLNs (Fig. 2.21).

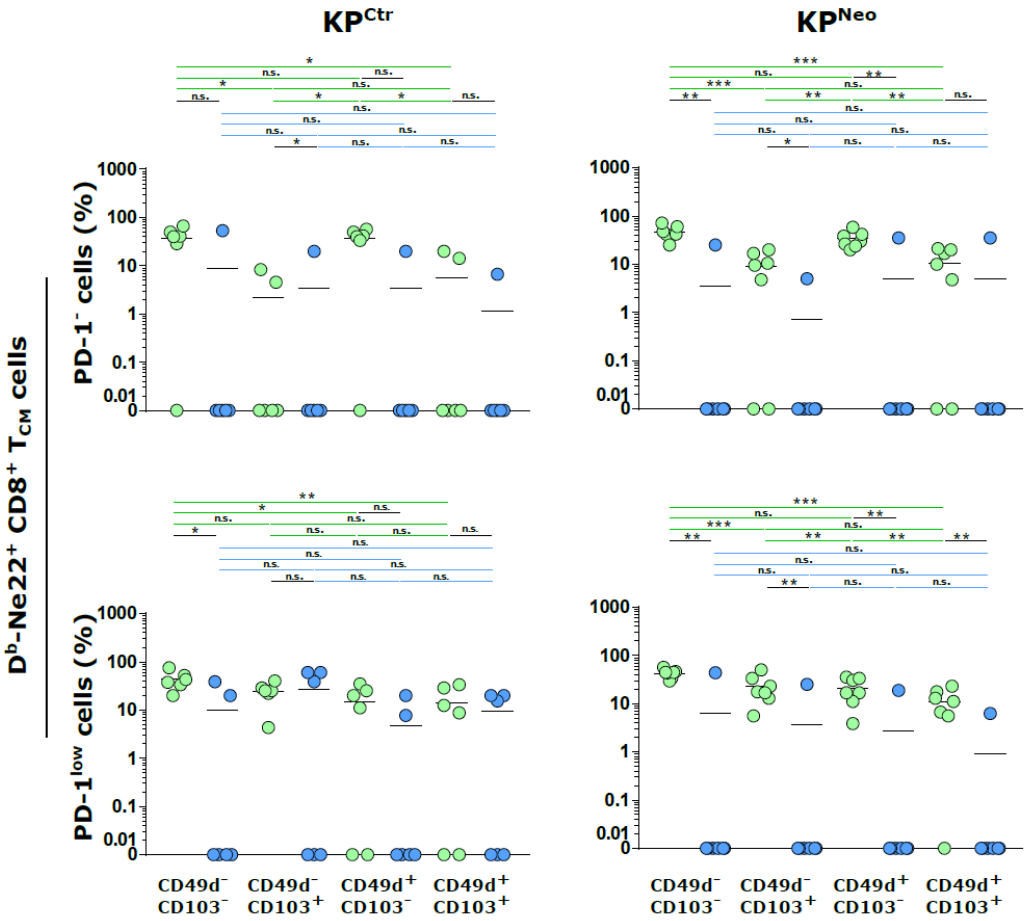

Figure 2.21 Subsets validation in Ne22-D^{b+}CD8$^+$ T$_{CM}$ cells from KP tumors and dLNs. Graphs showing the percentage of CD49d$^-$CD103$^-$, CD49d$^-$CD103$^+$, CD49d$^+$CD103$^-$ and CD49d$^+$CD103$^+$ cells on gated PD-1$^-$ or PD-1^{low} Ne22-D^{b+}CD8$^+$ T$_{CM}$ cells isolated from KP^{Ctr} and KP^{Neo} tumors and related dLNs. Each dot represents one single mouse. Statistics were calculated using Wilcoxon rank-sum test. *P < 0.05; **P < 0.01; ***P < 0.001; n.s.: not significant.

When we analysed D^b-Ne22$^+$CD8$^+$ T$_{EM}$ cells, they were found enriched among CD49d$^-$ CD103$^+$ PD-1^{high} and CD49d$^+$CD103$^+$PD-1^{high} subsets in the tumors (Fig. 2.22). Also in this case, we did not get differences in the abundancy of some subpopulations compared to the others.

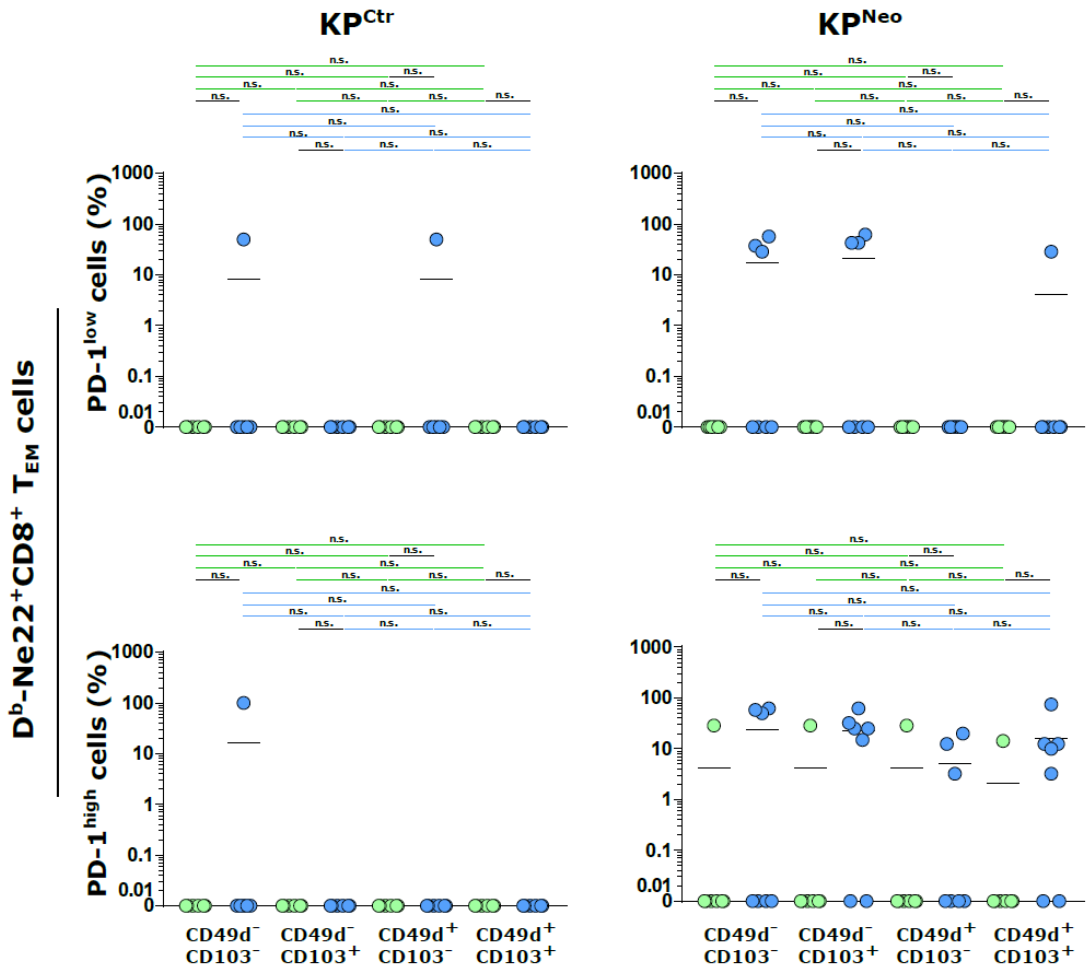

Figure 2.22. Subsets validation in Ne22-D^{b+}CD8$^+$ T$_{EM}$ cells from KP tumors and dLNs. Graphs showing the percentage of CD49d$^-$CD103$^-$, CD49d$^-$CD103$^+$, CD49d$^+$CD103$^-$ and CD49d$^+$CD103$^+$ cells on gated PD-1^{low} or PD-1^{high} Ne22-D^{b+}CD8$^+$ T$_{EM}$ cells isolated from KP^{Ctr} and KP^{Neo} tumors and related dLNs. Each dot represents one single mouse. Statistics were calculated using Wilcoxon rank-sum test. n.s.: not significant.

When we analysed the distribution of our immune subsets of interest in KP^{Ctr} compared with KP^{Neo} tumor, we observed that in the highly immunogenic one there was a higher frequency of CD103$^+$ subsets, corroborating what we detected in MC38.OVA colon cancer versus B16F10.OVA melanoma. In particular, we noticed that the percentage of CD49d$^-$CD103$^+$PD-1^{high} CD8$^+$ T$_{EM}$ TILs was significantly higher in KP^{Neo} compared to KP^{Ctr} tumor and we observed the same result among neoepitope-specific CD8$^+$ cells (Fig. 2.23 A-B). Overall, these data validate the hypothesis that tumors with different immunogenic potential could trigger the differentiation of distinct CD8$^+$ T cell subsets associated with different effector/memory properties.

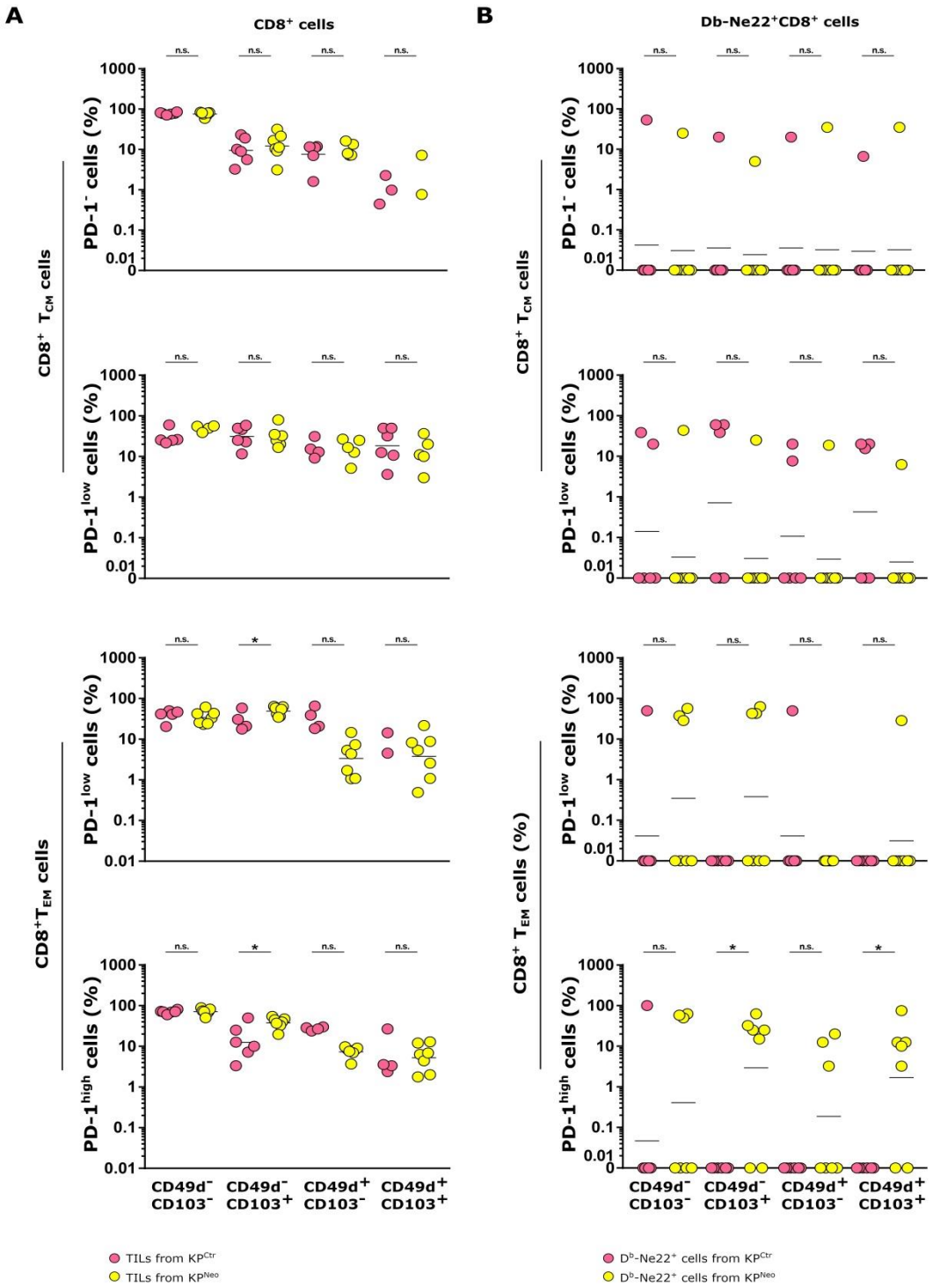

Figure 2.23. Comparison among TILs isolated from KP^{Ctr} and KP^{Neo} tumors. (**A**) Graphs showing the percentage of $CD49d^-CD103^-$, $CD49d^-CD103^+$, $CD49d^+CD103^-$ and $CD49d^+CD103^+$ cells on gated PD-1^- or PD-1^{low} $CD8^+$ T_{CM} and on gated PD-1^{low} or PD-1^{high} $CD8^+$ T_{EM} cells isolated from KP^{Ctr} and KP^{Neo} tumors. (**B**) Graphs showing the percentage of $CD49d^-CD103^-$, $CD49d^-CD103^+$, $CD49d^+CD103^-$ and $CD49d^+CD103^+$ cells on gated PD-1^- or PD-1^{low} Ne22-$D^{b+}CD8^+$ T_{CM} and on gated PD-1^{low} or PD-1^{high} Ne22-$D^{b+}CD8^+$ T_{EM} cells isolated from KP^{Ctr} and KP^{Neo} tumors. Each dot represents one mouse. Statistics were calculated using Wilcoxon rank-sum test. *$P < 0.05$; n.s.: not significant.

DISCUSSION

The immune system can suppress tumor development and progression through a process known as "cancer immunosurveillance" (*64*). Although many immune cells belonging both to the innate and adaptive immunity can be involved in this process, cytotoxic $CD8^+$ T lymphocytes play a particularly important role and are considered the major anti-tumor effector cells. Tumor cells express neoantigens that can be recognized by the immune cells. After antigen presentation, naïve $CD8^+$ T cells are activated, differentiate into effector cells and produce granzymes, perforin and other cytokines which induce death of tumor cells. Despite that, overtime tumor develops immunosuppressive mechanisms and protects itself from the elimination mediated by the immune cells (*111*). As a consequence, TILs accumulating in the tumor environment became exhausted and fail to arrest tumor progression. Exhausted TILs secrete low levels of effector cytokines and overexpress inhibitory receptors, such as PD-1, LAG-3 and TIM-3. Nowadays this receptors are therapeutic targets for checkpoint inhibition aimed to restore the anti-tumor activity of T cells (*112*). Moreover, to achieve long-lasting anti-tumor immunity, it is necessary to establish memory $CD8^+$ T cell response. In particular, several evidence demonstrated that antigen-specific T_{RM} cells mediate strong immunity against melanoma and other tumors (*113-115*), but the mechanisms by which these cells differentiate and determine enhanced anti-tumor immunity are still poorly understood. In this study we investigated: 1) how tumour antigenicity and immunogenicity influence $CD8^+$ T cell subset differentiation during cancer progression, 2) how the enrichment of some new $CD8^+$ T cell subpopulation in dLNs and TILs correlate with tumor rejection.

ScRNA-seq technologies allow the analysis of gene expression profiles at single-cell resolution, which has revolutionized the study of cell heterogeneity. Often, mRNA level is used as a substitute for protein amounts, however, correlation between mRNA and protein expression is usually weak (*116*). The general lack of correlation between transcriptome and proteome is due to the numerous and complex post-transcriptional steps involved in turning mRNA into protein. Another reason is that proteins may differ in their *in vivo* half-lives, as result of protein turnover that can be significantly different also among proteins with similar functions. To overcome these limits, we relied on the multi-omics BD Rhapsody system. Our combined analysis of surface markers and gene

expression profile at single cell level allowed the identification of different $CD8^+$ T cell sub-populations that we classified as transitional memory, $PD1^{low}$ cycling and $PD1^{high}$ T_{EX} and migratory/exhausted $CD8^+$ T cells. Although we do not know if there is a correlation between these newly identified subsets and tumor rejection, the validation of these sub-populations among neoantigen-specific $CD8^+$ T cells suggested that they could have a critical role against cancer development.

Many tumors arise in epithelial or other peripheral tissues (*117*) but only some $CD8^+$ T subsets are able to enter these compartments without clear inflammation (*118*). T_{RM} cells are a non-recirculating population permanently situated within several peripheral tissues, including skin (*119*), lung (*120*) and intestine (*121*). Although these cells are principally involved in the protection against local viral and bacterial infections (*122*), their role in the immune surveillance has also been demonstrated (*114, 123-125*). Our results revealed that when $CD8^+$ T cells are activated by a neoantigen such as Adpgk, specific immune cell subsets could upregulate the expression of CD49d and CD103 and differentiate in T_{RM} subsets. CD49d is an integrin involved in the rolling and adhesion steps of leucocyte transendothelial migration (*126*). Grau et al. demonstrated that memory $CD8^+$ T cells expressing high levels of CD49d, together with other integrins, such as CD29 and CD49a, play a key role in immune cell migration (*127, 128*). In particular, they showed that memory $CD8^+$ T cell recruitment into inflamed lung is CD49a/CD49d-dependent. In line with this, it is also known that CD49d is involved in the migration of T cells to the intestine, indeed one of the ligand of this integrin is the mucosal addressin cell adhesion molecule 1 (MAdCAM-1) (*129*). Ling et al. showed that in human colon carcinoma, $CD8^+$ TILs that are mainly localized in the tumor epithelium are $CD49d^+CD103^+$ (*130*). CD103 is an integrin involved in the localization of lymphocytes in the intraepithelial compartment (*131*), its ligand E-cadherin is expressed on epithelial cells. During cancer development and progression, CD103 expression is upregulated on $CD8^+$ T cells upon TRC engagement and exposure to TGF-β (*130*), that is abundant in the tumor microenvironment (*132*). CD103 can influence $CD8^+$ TIL function not only by promoting the adhesion to tumor cells, but also activating intracellular pathways that costimulate TCR signals (*133*). Moreover, several evidence suggest that this integrin has a role in the retention of TIL subpopulations in epithelial tissues through the interaction with the E-cadherin on

epithelial tumors (*134*). Park et al. demonstrated that T_{RM} cells are able to confer protection from melanoma development, playing a fundamental role in maintaining cancer-immune equilibrium. In line with this, many other groups demonstrated the active role of T_{RM} cells in anti-tumor activity (*80*, *135*). Of note, when we analysed $CD8^+$ T cell differentiation in response to tumour antigens with diverse expression levels and with different TCR affinity for the corresponding neoepitopes, we detected different frequency of $CD103^+CD8^+$ T cell subsets. We hypothesized that the expression of both CD103 and CD49d were strictly dependent on the antigen itself and its interaction with the TCR. Also, we confirmed higher expression of CD103 among D^b-Adpgk$^+$ $CD8^+$ T cells but not among K^b-SIINFEKL$^+$ $CD8^+$ T cells from MC38 and MC38.OVA tumors, respectively. In particular antigen-specific $CD49d^+CD103^+$ $PD1^{low}$ T_{CM}, $CD49d^+CD103^+$ $PD1^{low}$ and $CD49d^+CD103^+$ $PD1^{high}$ T_{EM} $CD8^+$ T cells were more abundant when the immune system was activated by a weak antigen compared to a strong one. By contrast, K^b-SIINFEKL$^+$ $CD8^+$ T cells showed higher frequencies of $CD49d^-CD103^-$ $PD1^{low}$ T_{CM}, $CD49d^-CD103^-$ $PD1^{low}$ and $CD49d^-CD103^+$-$PD1^{high}$ T_{EM} $CD8^+$ T cells. According to this, Adpgk triggered the activation of memory-like $CD8^+$ T subsets, whereas when the tumor cells expressed high levels of a neoepitope with a strong TCR affinity such as SIINFEKL, memory T subsets were less abundant, in favour of exhausted/cycling subsets. It is known that chronic exposure to high chronic antigen levels can lead to cell exhaustion (*40*). Clusters of $CD103^+CD8^+$ T_{RM}-like cells with differential expression of PD-1 and TIM-3 have been identified in human colon, breast and lung tumors (*136*-*138*) suggesting that $CD103^+CD8^+$ T_{RM} cells might become dysfunctional. In line with this, we observed that stronger antigens activate $CD8^+$ T cell differentiation towards the downregulation of CD103 and the acquisition of a T_{EX}-like phenotype.

Another important aspect that could drive $CD8^+$ T cell differentiation is the tumor immunogenicity. Indeed, when we analysed the frequency and distribution of $CD8^+$ T cell subsets isolated from KP^{Ctr} and KP^{Neo} tumors, we observed that highly immunogenic KP^{Neo} tumors showed higher frequency of $CD49d^-CD103^+$ T_{EM} cells compared to KP^{Ctr}. These data were also confirmed with the neoantigen-specific $CD8^+$ T cells, thus highlighting the important role of $CD103^+$ $CD8^+$ T cells in the protection against tumour progression. This is also in line with the fact that KP^{Neo} tumor growth

was slower compared to KP^{Ctr} ones, suggesting that $CD103^{+}CD8^{+}$ T subsets positively correlate with tumor rejection. It is interesting to note that, although we analysed the immune responses against a common neoepitope shared by both KP^{Ctr} and KP^{Neo} tumors, we could detect neoepitope-specific $CD8^{+}$ T cell response only against KP^{Neo} but not KP^{Ctr} tumor cells. We explained this phenomenon with the concept of epitope spreading. Epitope spreading is an immunologic process characterised by the amplification of T cell responses against an epitope different from the originally targeted one (*139*). In general, this phenomenon produces a more robust immune response to a given antigen. Indeed, TCR specific for a certain epitope recognizes the MHC-epitope complex on the surface of a tumor cell, that is destroyed by cytotoxic $CD8^{+}$ T cells and release its antigens. These antigens derived from dead tumor cells are processed by APC and presented to T cells with consequent expansion of polyclonal T cell responses with different specificities. When a tumor expresses a lot of neoantigens, such as KP^{Neo} tumor, the magnitude of this process is consistent and determines a more powerful immune response. Epitope spreading and consequent expansion of newly generated T cells contribute to the efficacy of several immunotherapeutic approaches (*140-143*).

In future, we plan to perform immunohistochemical analysis of the expression of CD49d and CD103 on $CD8^{+}$ TILs within mouse colon carcinoma sections in order to understand the spatial localization of our sub-populations of interest. We will try to expand the $CD8^{+}$ T cell subsets with specific target antigens to generate a number of cells sufficient to perform functional assays and adoptive transfer T cell therapy. Also, we will perform in vivo experiments with immune checkpoint blockade in order to understand if treatment of tumors with anti-PD-1 immunotherapy can influence the abundance of some $CD8^{+}$ T cell sub-populations compared to others and compared to non-treated tumors.

In conclusions, our data show that $CD8^{+}$ T cell differentiation is strongly influenced by the antigen that elicits the immune response. When the antigen expression level is low and its affinity for the TCR is low/moderate, $CD8^{+}$ T cell subsets differentiate towards a T_{RM} memory-like phenotype and positively correlate with tumor rejection. Several evidence indicate that T_{RM} cells are key players in the inhibition of cancer growth and are often associated to improved outcomes (*144, 145*). Also, these cells show better

cytotoxic potential and effector functions when compared with $CD103^-$ TILs, indeed T_{RM} isolated from different tumor samples express higher amount of perforin and granzyme (*146*). However, T_{RM} cells belonging to the same tumor could be very heterogeneous and have a distinct protective potential. According to this, the factors that determines the diversification of T_{RM} subsets and their function require further investigation. In the future, it will be important to explore and validate the presence of our newly identified subsets also in human cancer samples, elucidating how the new subsets correlate with patient survival and active immune responses to cancer.

MATERIALS AND METHODS

Mice

C57BL/6J male mice were purchased from Charles River Laboratories and housed in Molecular Biotechnology Center (MBC) (Turin University) specific pathogen free (SPF) Animal Facility. 8-12 weeks old mice were used for the experiments. Live animal experiments were done in accordance with the guidelines of Italian and European Veterinary Department.

Tumor cell lines

Mouse colon cancer cell lines MC38, MC38.OVA and mouse melanoma cell line B16F10.OVA were purchased at ATTC. Mouse lung carcinoma cell line KP has been isolated from C57BL/6 K-ras$^{LSLG12D/+}$; p53$^{fl/fl}$ mice (*147*). The line was kindly provided by Dr. Tyler Jacks (Massachusetts Institute of Technology, Cambridge, USA). Mlh1 knockout clones were generated by Crispr Cas9 based technology using 2 single guide RNAs (sgRNA) targeting Mlh1 exon 5 as described in (*148*). Early passage cancer cells were kept in culture under standard condition of 37°C and 5% CO_2 in DMEM medium supplemented with 1% pen/strep (100 U/mL and 100 µg/mL), 1% L-glutamine (50mM) and 10% FBS (all from GIBCO).

In vivo tumor progression

Cells were collected during their exponential growth phase. $2x10^5$ MC38 or MC38.OVA, $6x10^5$ B16F10.OVA and $5x10^5$ KP cells were s.c. injected into mice in order to induce the tumor formation. Tumor growth was monitored every 3 to 4 days using a caliper. Mice carrying subcutaneous tumors were sacrificed at the indicated time points, and the tumors and the draining lymph nodes were collected. Tumor volume was calculated as (tumor size width)^2 x (length) / 2, where the length was the longer of the 2 measurements.

Lymphocyte isolation

Tumors and draining lymph nodes were harvested at the indicated time points. Single-cell suspensions of lymphocytes from lymph nodes were generated and cell number was determined. Tumor-infiltrating lymphocytes were enriched by Percoll gradient before

labelling. Cell suspensions were prepared in phosphate-buffered saline (PBS)–0.5% bovine serum albumin (BSA) and 2 mM EDTA.

Flow cytometry and cell sorting

Cells were labelled according to the experiment with anti-CD44 (clone IM-7), anti-CD62L (clone MEL-14), anti-CD8 (clone 53-6.7), anti-TCRβ (clone H57-597), anti-CD103 (clone M290), anti-PD-1 (clone J43), anti-CD122 (clone TM-β1), anti-CD49d (clone R1-2). Cells were fixed with 1% paraformaldehyde. Fc receptors were blocked with the CD16/CD32 (2.4.G2) monoclonal antibody. Dead cells were stained with cell death dyes (BD) according to the manufacturer's instructions. Phenotypic characterization of lymphocytes was performed using BD LSRFortessa X-20 and sorted with BD FACSAria III. The data were analysed with FlowJo 10.7.2 software.

Single-cell RNA and Ab-O sequencing by BD Rhapsody system

Targeted scRNA-seq, Ab-seq and Sample Tag-seq were performed according to the manufacturer's instructions using the BD Rhapsody Express system (BD Biosciences). Briefly, lymphocytes isolated from tumors and draining lymph modes were labelled for 30 min on ice with 38 Ab-O and a different Sample Tag for each sample. Each Ab-O is an oligonucleotide conjugated antibody that contains an Ab-UMI and a polyA tail for bead capture, PCR amplification, and library generation. Sample Tag consists of a unique 45-nucleotide barcode sequence conjugated with an antibody and associated with a universal PCR handle and a poly(A) tail necessary for the binding to the beads. The use of Sample Tag allows the discrimination of the different samples. After the staining, cells were counted and resuspended in 650 μL of cold sample buffer for loading on a BD Rhapsody cartridge. Each single cell was settled into a microwell. This was followed by cell lysis, bead retrieval, cDNA synthesis, template switching, Klenow extension, and library preparation. Libraries quantification and quality assessment were achieved by Qubit fluorometric assay using dsDNA High Sensitivity Assay Kit (Invitrogen) or by Bioanalyzer Agilent 2100 System using a High Sensitivity DNA chip. Libraries were equimolarly combined and the final pool was spiked with 20% PhiX control DNA to increase the sequence complexity and subsequently sequenced (75 bp × 75 bp paired-end) on NovaSeq 6000 System (Illumina).

Single-cell RNA-seq and Ab-O data analysis

Single-cell RNA-seq and Ab-seq data were generated targeting 662 genes and using 38 Ab-O. RNA-seq and Ab-seq matrixes were analysed using SeqGeq software v1.6. Normalization to improve data comparability (10000 event count/cell) was performed. It was followed by cell quality control to remove outlier events which might represent empty wells, or doublets, and gene quality control to remove dimly expressed genes and genes expressed in most cells. Then, selection of the highly dispersed features was performed, in order to select the parameters with the highest level of variance that allows to separate biologically relevant populations within data matrices. Highly dispersed features were used as an input to perform dimensionality reduction based on the principal component analysis (PCA) and to create t-distributed stochastic neighbour embedding (t-SNE) projection. Uniform Manifold Approximation and Projection (UMAP) dimensionality reduction was also performed. Data clustering has been carried out by using the PhenoGraph algorithm, which is based on the construction of a nearest-neighbour graph to capture the phenotypic relatedness of high-dimensional data points and then it applies the Louvain graph partition algorithm to dissect the nearest-neighbour graph into phenotypically coherent subpopulations. Differential expression analysis was calculated between tumors and dLNs compartments through the use of volcano plots (fold change > or < 1,5, q value < 0,05) or through the iCellR plugin between data clusters (fold change > or < 1,2, q value < 0,05). Heatmaps illustrating expression patterns between populations, genes or proteins of interest were created using the ViolinBox plugin.

REFERENCES

1. J. S. Marshall, R. Warrington, W. Watson, H. L. Kim, An introduction to immunology and immunopathology. *Allergy Asthma Clin Immunol* 14, 49 (2018).
2. J. B. Chung, M. Silverman, J. G. Monroe, Transitional B cells: step by step towards immune competence. *Trends Immunol* 24, 343-349 (2003).
3. H. P. Savage, N. Baumgarth, Characteristics of natural antibody-secreting cells. *Ann N Y Acad Sci* 1362, 132-142 (2015).
4. D. J. Chung *et al.*, Disease- and Therapy-Specific Impact on Humoral Immune Responses to COVID-19 Vaccination in Hematologic Malignancies. *Blood Cancer Discov* 2, 568-576 (2021).
5. R. N. Germain, T-cell development and the CD4-CD8 lineage decision. *Nat Rev Immunol* 2, 309-322 (2002).
6. H. von Boehmer, Aspects of lymphocyte developmental biology. *Immunol Today* 18, 260-262 (1997).
7. G. J. Nossal, Negative selection of lymphocytes. *Cell* 76, 229-239 (1994).
8. R. W. Dutton, L. M. Bradley, S. L. Swain, T cell memory. *Annu Rev Immunol* 16, 201-223 (1998).
9. M. Ruterbusch, K. B. Pruner, L. Shehata, M. Pepper, In Vivo CD4(+) T Cell Differentiation and Function: Revisiting the Th1/Th2 Paradigm. *Annu Rev Immunol* 38, 705-725 (2020).
10. F. Annunziato, C. Romagnani, S. Romagnani, The 3 major types of innate and adaptive cell-mediated effector immunity. *J Allergy Clin Immunol* 135, 626-635 (2015).
11. L. Zhou, M. M. Chong, D. R. Littman, Plasticity of CD4+ T cell lineage differentiation. *Immunity* 30, 646-655 (2009).
12. Y. Kanno, G. Vahedi, K. Hirahara, K. Singleton, J. J. O'Shea, Transcriptional and epigenetic control of T helper cell specification: molecular mechanisms underlying commitment and plasticity. *Annu Rev Immunol* 30, 707-731 (2012).
13. D. Masopust, J. M. Schenkel, The integration of T cell migration, differentiation and function. *Nat Rev Immunol* 13, 309-320 (2013).
14. S. M. Kaech, W. Cui, Transcriptional control of effector and memory CD8+ T cell differentiation. *Nat Rev Immunol* 12, 749-761 (2012).
15. E. J. Wherry, R. Ahmed, Memory CD8 T-cell differentiation during viral infection. *J Virol* 78, 5535-5545 (2004).
16. S. M. Kaech, E. J. Wherry, R. Ahmed, Effector and memory T-cell differentiation: implications for vaccine development. *Nat Rev Immunol* 2, 251-262 (2002).
17. C. Gerlach *et al.*, One naive T cell, multiple fates in CD8+ T cell differentiation. *J Exp Med* 207, 1235-1246 (2010).
18. M. Pigliucci, C. J. Murren, C. D. Schlichting, Phenotypic plasticity and evolution by genetic assimilation. *J Exp Biol* 209, 2362-2367 (2006).

19. D. Homann, L. Teyton, M. B. Oldstone, Differential regulation of antiviral T-cell immunity results in stable CD8+ but declining CD4+ T-cell memory. *Nat Med* 7, 913-919 (2001).
20. D. Masopust *et al.*, Activated primary and memory CD8 T cells migrate to nonlymphoid tissues regardless of site of activation or tissue of origin. *J Immunol* 172, 4875-4882 (2004).
21. D. L. Barber, E. J. Wherry, R. Ahmed, Cutting edge: rapid in vivo killing by memory CD8 T cells. *J Immunol* 171, 27-31 (2003).
22. A. Lalvani *et al.*, Rapid effector function in CD8+ memory T cells. *J Exp Med* 186, 859-865 (1997).
23. V. P. Badovinac, B. B. Porter, J. T. Harty, Programmed contraction of CD8(+) T cells after infection. *Nat Immunol* 3, 619-626 (2002).
24. F. Sallusto, D. Lenig, R. Forster, M. Lipp, A. Lanzavecchia, Two subsets of memory T lymphocytes with distinct homing potentials and effector functions. *Nature* 401, 708-712 (1999).
25. E. J. Wherry *et al.*, Lineage relationship and protective immunity of memory CD8 T cell subsets. *Nat Immunol* 4, 225-234 (2003).
26. J. A. Olson, C. McDonald-Hyman, S. C. Jameson, S. E. Hamilton, Effector-like CD8(+) T cells in the memory population mediate potent protective immunity. *Immunity* 38, 1250-1260 (2013).
27. N. S. Joshi *et al.*, Inflammation directs memory precursor and short-lived effector CD8(+) T cell fates via the graded expression of T-bet transcription factor. *Immunity* 27, 281-295 (2007).
28. R. L. Rutishauser *et al.*, Transcriptional repressor Blimp-1 promotes CD8(+) T cell terminal differentiation and represses the acquisition of central memory T cell properties. *Immunity* 31, 296-308 (2009).
29. X. Jiang *et al.*, Skin infection generates non-migratory memory CD8+ T(RM) cells providing global skin immunity. *Nature* 483, 227-231 (2012).
30. L. K. Mackay *et al.*, The developmental pathway for CD103(+)CD8+ tissue-resident memory T cells of skin. *Nat Immunol* 14, 1294-1301 (2013).
31. L. K. Mackay *et al.*, Cutting edge: CD69 interference with sphingosine-1-phosphate receptor function regulates peripheral T cell retention. *J Immunol* 194, 2059-2063 (2015).
32. L. K. Mackay *et al.*, T-box Transcription Factors Combine with the Cytokines TGF-beta and IL-15 to Control Tissue-Resident Memory T Cell Fate. *Immunity* 43, 1101-1111 (2015).
33. C. N. Skon *et al.*, Transcriptional downregulation of S1pr1 is required for the establishment of resident memory CD8+ T cells. *Nat Immunol* 14, 1285-1293 (2013).
34. N. Zhang, M. J. Bevan, Transforming growth factor-beta signaling controls the formation and maintenance of gut-resident memory T cells by regulating migration and retention. *Immunity* 39, 687-696 (2013).

35. M. E. Hoekstra, S. V. Vijver, T. N. Schumacher, Modulation of the tumor micro-environment by CD8(+) T cell-derived cytokines. *Curr Opin Immunol* 69, 65-71 (2021).
36. D. Masopust, V. Vezys, E. J. Wherry, D. L. Barber, R. Ahmed, Cutting edge: gut microenvironment promotes differentiation of a unique memory CD8 T cell population. *J Immunol* 176, 2079-2083 (2006).
37. J. M. Schenkel, K. A. Fraser, V. Vezys, D. Masopust, Sensing and alarm function of resident memory CD8(+) T cells. *Nat Immunol* 14, 509-513 (2013).
38. J. M. Schenkel *et al.*, T cell memory. Resident memory CD8 T cells trigger protective innate and adaptive immune responses. *Science* 346, 98-101 (2014).
39. C. Gerlach *et al.*, The Chemokine Receptor CX3CR1 Defines Three Antigen-Experienced CD8 T Cell Subsets with Distinct Roles in Immune Surveillance and Homeostasis. *Immunity* 45, 1270-1284 (2016).
40. E. J. Wherry, T cell exhaustion. *Nat Immunol* 12, 492-499 (2011).
41. E. J. Wherry, J. N. Blattman, K. Murali-Krishna, R. van der Most, R. Ahmed, Viral persistence alters CD8 T-cell immunodominance and tissue distribution and results in distinct stages of functional impairment. *J Virol* 77, 4911-4927 (2003).
42. M. Hashimoto *et al.*, CD8 T Cell Exhaustion in Chronic Infection and Cancer: Opportunities for Interventions. *Annu Rev Med* 69, 301-318 (2018).
43. E. J. Wherry, M. Kurachi, Molecular and cellular insights into T cell exhaustion. *Nat Rev Immunol* 15, 486-499 (2015).
44. C. Paluch, A. M. Santos, C. Anzilotti, R. J. Cornall, S. J. Davis, Immune Checkpoints as Therapeutic Targets in Autoimmunity. *Front Immunol* 9, 2306 (2018).
45. M. Matloubian, R. J. Concepcion, R. Ahmed, CD4+ T cells are required to sustain CD8+ cytotoxic T-cell responses during chronic viral infection. *J Virol* 68, 8056-8063 (1994).
46. M. Quigley *et al.*, Transcriptional analysis of HIV-specific CD8+ T cells shows that PD-1 inhibits T cell function by upregulating BATF. *Nat Med* 16, 1147-1151 (2010).
47. C. M. Bucks, J. A. Norton, A. C. Boesteanu, Y. M. Mueller, P. D. Katsikis, Chronic antigen stimulation alone is sufficient to drive CD8+ T cell exhaustion. *J Immunol* 182, 6697-6708 (2009).
48. S. D. Blackburn *et al.*, Coregulation of CD8+ T cell exhaustion by multiple inhibitory receptors during chronic viral infection. *Nat Immunol* 10, 29-37 (2009).
49. L. Trautmann *et al.*, Upregulation of PD-1 expression on HIV-specific CD8+ T cells leads to reversible immune dysfunction. *Nat Med* 12, 1198-1202 (2006).
50. C. L. Day *et al.*, PD-1 expression on HIV-specific T cells is associated with T-cell exhaustion and disease progression. *Nature* 443, 350-354 (2006).

51. B. Youngblood *et al.*, Chronic virus infection enforces demethylation of the locus that encodes PD-1 in antigen-specific CD8(+) T cells. *Immunity* 35, 400-412 (2011).
52. M. E. Keir, M. J. Butte, G. J. Freeman, A. H. Sharpe, PD-1 and its ligands in tolerance and immunity. *Annu Rev Immunol* 26, 677-704 (2008).
53. B. H. Zinselmeyer *et al.*, PD-1 promotes immune exhaustion by inducing antiviral T cell motility paralysis. *J Exp Med* 210, 757-774 (2013).
54. A. Ribas, J. D. Wolchok, Cancer immunotherapy using checkpoint blockade. *Science* 359, 1350-1355 (2018).
55. M. A. Paley *et al.*, Progenitor and terminal subsets of CD8+ T cells cooperate to contain chronic viral infection. *Science* 338, 1220-1225 (2012).
56. S. D. Blackburn, H. Shin, G. J. Freeman, E. J. Wherry, Selective expansion of a subset of exhausted CD8 T cells by alphaPD-L1 blockade. *Proc Natl Acad Sci U S A* 105, 15016-15021 (2008).
57. M. M. Gubin, M. N. Artyomov, E. R. Mardis, R. D. Schreiber, Tumor neoantigens: building a framework for personalized cancer immunotherapy. *J Clin Invest* 125, 3413-3421 (2015).
58. L. Schuchter *et al.*, A prognostic model for predicting 10-year survival in patients with primary melanoma. The Pigmented Lesion Group. *Ann Intern Med* 125, 369-375 (1996).
59. S. Wagner, C. S. Mullins, M. Linnebacher, Colorectal cancer vaccines: Tumor-associated antigens vs neoantigens. *World J Gastroenterol* 24, 5418-5432 (2018).
60. B. Heemskerk, P. Kvistborg, T. N. Schumacher, The cancer antigenome. *EMBO J* 32, 194-203 (2013).
61. T. N. Schumacher, R. D. Schreiber, Neoantigens in cancer immunotherapy. *Science* 348, 69-74 (2015).
62. D. Hamann *et al.*, Phenotypic and functional separation of memory and effector human CD8+ T cells. *J Exp Med* 186, 1407-1418 (1997).
63. N. Lee, L. R. Zakka, M. C. Mihm, Jr., T. Schatton, Tumour-infiltrating lymphocytes in melanoma prognosis and cancer immunotherapy. *Pathology* 48, 177-187 (2016).
64. R. D. Schreiber, L. J. Old, M. J. Smyth, Cancer immunoediting: integrating immunity's roles in cancer suppression and promotion. *Science* 331, 1565-1570 (2011).
65. F. R. Greten, S. I. Grivennikov, Inflammation and Cancer: Triggers, Mechanisms, and Consequences. *Immunity* 51, 27-41 (2019).
66. M. D. Vesely, M. H. Kershaw, R. D. Schreiber, M. J. Smyth, Natural innate and adaptive immunity to cancer. *Annu Rev Immunol* 29, 235-271 (2011).
67. A. Mantovani, P. Allavena, A. Sica, F. Balkwill, Cancer-related inflammation. *Nature* 454, 436-444 (2008).

68. M. J. Gooden, G. H. de Bock, N. Leffers, T. Daemen, H. W. Nijman, The prognostic influence of tumour-infiltrating lymphocytes in cancer: a systematic review with meta-analysis. *Br J Cancer* 105, 93-103 (2011).
69. L. Zhang *et al.*, Intratumoral T cells, recurrence, and survival in epithelial ovarian cancer. *N Engl J Med* 348, 203-213 (2003).
70. F. Maibach, H. Sadozai, S. M. Seyed Jafari, R. E. Hunger, M. Schenk, Tumor-Infiltrating Lymphocytes and Their Prognostic Value in Cutaneous Melanoma. *Front Immunol* 11, 2105 (2020).
71. W. H. Clark, Jr. *et al.*, Model predicting survival in stage I melanoma based on tumor progression. *J Natl Cancer Inst* 81, 1893-1904 (1989).
72. Z. Mei *et al.*, Tumour-infiltrating inflammation and prognosis in colorectal cancer: systematic review and meta-analysis. *Br J Cancer* 110, 1595-1605 (2014).
73. H. Elomaa *et al.*, Prognostic significance of spatial and density analysis of T lymphocytes in colorectal cancer. *Br J Cancer* 127, 514-523 (2022).
74. W. T. Hwang, S. F. Adams, E. Tahirovic, I. S. Hagemann, G. Coukos, Prognostic significance of tumor-infiltrating T cells in ovarian cancer: a meta-analysis. *Gynecol Oncol* 124, 192-198 (2012).
75. P. C. Yu, D. Long, C. C. Liao, S. Zhang, Association between density of tumor-infiltrating lymphocytes and prognoses of patients with gastric cancer. *Medicine (Baltimore)* 97, e11387 (2018).
76. J. R. Webb, K. Milne, B. H. Nelson, PD-1 and CD103 Are Widely Coexpressed on Prognostically Favorable Intraepithelial CD8 T Cells in Human Ovarian Cancer. *Cancer Immunol Res* 3, 926-935 (2015).
77. Y. Nose *et al.*, The tissue-resident marker CD103 on peripheral blood T cells predicts responses to anti-PD-1 therapy in gastric cancer. *Cancer Immunol Immunother* 72, 169-181 (2023).
78. Y. Kim, Y. Shin, G. H. Kang, Prognostic significance of CD103+ immune cells in solid tumor: a systemic review and meta-analysis. *Sci Rep* 9, 3808 (2019).
79. J. R. Webb, K. Milne, P. Watson, R. J. Deleeuw, B. H. Nelson, Tumor-infiltrating lymphocytes expressing the tissue resident memory marker CD103 are associated with increased survival in high-grade serous ovarian cancer. *Clin Cancer Res* 20, 434-444 (2014).
80. Z. Q. Wang *et al.*, CD103 and Intratumoral Immune Response in Breast Cancer. *Clin Cancer Res* 22, 6290-6297 (2016).
81. M. H. Park, S. Y. Kwon, J. E. Choi, G. Gong, Y. K. Bae, Intratumoral CD103-positive tumour-infiltrating lymphocytes are associated with favourable prognosis in patients with triple-negative breast cancer. *Histopathology* 77, 560-569 (2020).
82. W. Hu, R. Sun, L. Chen, X. Zheng, J. Jiang, Prognostic significance of resident CD103(+)CD8(+)T cells in human colorectal cancer tissues. *Acta Histochem* 121, 657-663 (2019).

83. E. J. de Ruiter, M. L. Ooft, L. A. Devriese, S. M. Willems, The prognostic role of tumor infiltrating T-lymphocytes in squamous cell carcinoma of the head and neck: A systematic review and meta-analysis. *Oncoimmunology* 6, e1356148 (2017).
84. D. Borsetto *et al.*, Prognostic Significance of CD4+ and CD8+ Tumor-Infiltrating Lymphocytes in Head and Neck Squamous Cell Carcinoma: A Meta-Analysis. *Cancers (Basel)* 13, (2021).
85. A. Giatromanolaki *et al.*, Programmed death-1 receptor (PD-1) and PD-ligand-1 (PD-L1) expression in non-small cell lung cancer and the immune-suppressive effect of anaerobic glycolysis. *Med Oncol* 36, 76 (2019).
86. S. J. Russell, K. W. Peng, J. C. Bell, Oncolytic virotherapy. *Nat Biotechnol* 30, 658-670 (2012).
87. R. H. Andtbacka *et al.*, Talimogene Laherparepvec Improves Durable Response Rate in Patients With Advanced Melanoma. *J Clin Oncol* 33, 2780-2788 (2015).
88. M. B. Atkins, L. Kunkel, M. Sznol, S. A. Rosenberg, High-dose recombinant interleukin-2 therapy in patients with metastatic melanoma: long-term survival update. *Cancer J Sci Am* 6 Suppl 1, S11-14 (2000).
89. G. Fyfe *et al.*, Results of treatment of 255 patients with metastatic renal cell carcinoma who received high-dose recombinant interleukin-2 therapy. *J Clin Oncol* 13, 688-696 (1995).
90. P. Solal-Celigny *et al.*, Recombinant interferon alfa-2b combined with a regimen containing doxorubicin in patients with advanced follicular lymphoma. Groupe d'Etude des Lymphomes de l'Adulte. *N Engl J Med* 329, 1608-1614 (1993).
91. H. M. Golomb *et al.*, Alpha-2 interferon therapy of hairy-cell leukemia: a multicenter study of 64 patients. *J Clin Oncol* 4, 900-905 (1986).
92. J. M. Kirkwood *et al.*, Interferon Alfa-2b Adjuvant Therapy of High-Risk Resected Cutaneous Melanoma: The Eastern Cooperative Oncology Group Trial EST 1684. *J Clin Oncol* 41, 425-435 (2023).
93. S. A. Rosenberg, N. P. Restifo, J. C. Yang, R. A. Morgan, M. E. Dudley, Adoptive cell transfer: a clinical path to effective cancer immunotherapy. *Nat Rev Cancer* 8, 299-308 (2008).
94. M. V. Maus *et al.*, Adoptive immunotherapy for cancer or viruses. *Annu Rev Immunol* 32, 189-225 (2014).
95. C. H. June, S. R. Riddell, T. N. Schumacher, Adoptive cellular therapy: a race to the finish line. *Sci Transl Med* 7, 280ps287 (2015).
96. T. N. Schumacher, T-cell-receptor gene therapy. *Nat Rev Immunol* 2, 512-519 (2002).
97. G. Gross, T. Waks, Z. Eshhar, Expression of immunoglobulin-T-cell receptor chimeric molecules as functional receptors with antibody-type specificity. *Proc Natl Acad Sci U S A* 86, 10024-10028 (1989).
98. S. L. Maude, E. J. Shpall, S. A. Grupp, Chimeric antigen receptor T-cell therapy for ALL. *Hematology Am Soc Hematol Educ Program* 2014, 559-564 (2014).

99. F. S. Hodi *et al.*, Improved survival with ipilimumab in patients with metastatic melanoma. *N Engl J Med* 363, 711-723 (2010).
100. C. Robert *et al.*, Nivolumab in previously untreated melanoma without BRAF mutation. *N Engl J Med* 372, 320-330 (2015).
101. D. T. Le, D. M. Pardoll, E. M. Jaffee, Cellular vaccine approaches. *Cancer J* 16, 304-310 (2010).
102. A. M. D'Alise *et al.*, Adenoviral-based vaccine promotes neoantigen-specific CD8(+) T cell stemness and tumor rejection. *Sci Transl Med* 14, eabo7604 (2022).
103. H. Khong, W. W. Overwijk, Adjuvants for peptide-based cancer vaccines. *J Immunother Cancer* 4, 56 (2016).
104. A. Tiptiri-Kourpeti, K. Spyridopoulou, A. Pappa, K. Chlichlia, DNA vaccines to attack cancer: Strategies for improving immunogenicity and efficacy. *Pharmacol Ther* 165, 32-49 (2016).
105. G. Wu, L. Nie, W. Zhang, Integrative analyses of posttranscriptional regulation in the yeast Saccharomyces cerevisiae using transcriptomic and proteomic data. *Curr Microbiol* 57, 18-22 (2008).
106. A. Beyer, J. Hollunder, H. P. Nasheuer, T. Wilhelm, Post-transcriptional expression regulation in the yeast Saccharomyces cerevisiae on a genomic scale. *Mol Cell Proteomics* 3, 1083-1092 (2004).
107. V. Russo, N. Brasu, L. Pace, Combined Measurement of RNA and Protein Expression on a Single-Cell Level. *Methods Mol Biol* 2386, 263-288 (2022).
108. S. Slovin *et al.*, Single-Cell RNA Sequencing Analysis: A Step-by-Step Overview. *Methods Mol Biol* 2284, 343-365 (2021).
109. M. Yadav *et al.*, Predicting immunogenic tumour mutations by combining mass spectrometry and exome sequencing. *Nature* 515, 572-576 (2014).
110. L. Pace *et al.*, Regulatory T cells increase the avidity of primary CD8+ T cell responses and promote memory. *Science* 338, 532-536 (2012).
111. T. L. Whiteside, Immune responses to malignancies. *J Allergy Clin Immunol* 125, S272-283 (2010).
112. D. M. Pardoll, The blockade of immune checkpoints in cancer immunotherapy. *Nat Rev Cancer* 12, 252-264 (2012).
113. B. T. Malik *et al.*, Resident memory T cells in the skin mediate durable immunity to melanoma. *Sci Immunol* 2, (2017).
114. M. Enamorado *et al.*, Enhanced anti-tumour immunity requires the interplay between resident and circulating memory CD8(+) T cells. *Nat Commun* 8, 16073 (2017).
115. M. Nizard *et al.*, Induction of resident memory T cells enhances the efficacy of cancer vaccine. *Nat Commun* 8, 15221 (2017).
116. D. Greenbaum, C. Colangelo, K. Williams, M. Gerstein, Comparing protein abundance and mRNA expression levels on a genomic scale. *Genome Biol* 4, 117 (2003).

117. J. Ferlay *et al.*, Cancer incidence and mortality worldwide: sources, methods and major patterns in GLOBOCAN 2012. *Int J Cancer* 136, E359-386 (2015).
118. S. C. Jameson, D. Masopust, Understanding Subset Diversity in T Cell Memory. *Immunity* 48, 214-226 (2018).
119. T. Gebhardt, F. R. Carbone, Immunology: A helpers' guide to infection. *Nature* 462, 418-419 (2009).
120. B. Piet *et al.*, CD8(+) T cells with an intraepithelial phenotype upregulate cytotoxic function upon influenza infection in human lung. *J Clin Invest* 121, 2254-2263 (2011).
121. D. Masopust *et al.*, Dynamic T cell migration program provides resident memory within intestinal epithelium. *J Exp Med* 207, 553-564 (2010).
122. S. N. Mueller, L. K. Mackay, Tissue-resident memory T cells: local specialists in immune defence. *Nat Rev Immunol* 16, 79-89 (2016).
123. F. Djenidi *et al.*, CD8+CD103+ tumor-infiltrating lymphocytes are tumor-specific tissue-resident memory T cells and a prognostic factor for survival in lung cancer patients. *J Immunol* 194, 3475-3486 (2015).
124. F. Mami-Chouaib *et al.*, Resident memory T cells, critical components in tumor immunology. *J Immunother Cancer* 6, 87 (2018).
125. S. L. Park, T. Gebhardt, L. K. Mackay, Tissue-Resident Memory T Cells in Cancer Immunosurveillance. *Trends Immunol* 40, 735-747 (2019).
126. C. Berlin *et al.*, alpha 4 integrins mediate lymphocyte attachment and rolling under physiologic flow. *Cell* 80, 413-422 (1995).
127. M. Grau *et al.*, Antigen-Induced but Not Innate Memory CD8 T Cells Express NKG2D and Are Recruited to the Lung Parenchyma upon Viral Infection. *J Immunol* 200, 3635-3646 (2018).
128. S. Nourshargh, R. Alon, Leukocyte migration into inflamed tissues. *Immunity* 41, 694-707 (2014).
129. C. Berlin *et al.*, Alpha 4 beta 7 integrin mediates lymphocyte binding to the mucosal vascular addressin MAdCAM-1. *Cell* 74, 185-195 (1993).
130. K. L. Ling *et al.*, Modulation of CD103 expression on human colon carcinoma-specific CTL. *J Immunol* 178, 2908-2915 (2007).
131. M. P. Schon *et al.*, Mucosal T lymphocyte numbers are selectively reduced in integrin alpha E (CD103)-deficient mice. *J Immunol* 162, 6641-6649 (1999).
132. C. H. Stuelten, Y. E. Zhang, Transforming Growth Factor-beta: An Agent of Change in the Tumor Microenvironment. *Front Cell Dev Biol* 9, 764727 (2021).
133. A. Le Floc'h *et al.*, Minimal engagement of CD103 on cytotoxic T lymphocytes with an E-cadherin-Fc molecule triggers lytic granule polarization via a phospholipase Cgamma-dependent pathway. *Cancer Res* 71, 328-338 (2011).
134. K. Franciszkiewicz *et al.*, CD103 or LFA-1 engagement at the immune synapse between cytotoxic T cells and tumor cells promotes maturation and regulates T-cell effector functions. *Cancer Res* 73, 617-628 (2013).

135. J. Edwards *et al.*, CD103(+) Tumor-Resident CD8(+) T Cells Are Associated with Improved Survival in Immunotherapy-Naive Melanoma Patients and Expand Significantly During Anti-PD-1 Treatment. *Clin Cancer Res* 24, 3036-3045 (2018).
136. X. Guo *et al.*, Global characterization of T cells in non-small-cell lung cancer by single-cell sequencing. *Nat Med* 24, 978-985 (2018).
137. L. Zhang *et al.*, Lineage tracking reveals dynamic relationships of T cells in colorectal cancer. *Nature* 564, 268-272 (2018).
138. B. Bengsch *et al.*, Epigenomic-Guided Mass Cytometry Profiling Reveals Disease-Specific Features of Exhausted CD8 T Cells. *Immunity* 48, 1029-1045 e1025 (2018).
139. C. L. Vanderlugt, S. D. Miller, Epitope spreading in immune-mediated diseases: implications for immunotherapy. *Nat Rev Immunol* 2, 85-95 (2002).
140. M. L. Disis *et al.*, Generation of T-cell immunity to the HER-2/neu protein after active immunization with HER-2/neu peptide-based vaccines. *J Clin Oncol* 20, 2624-2632 (2002).
141. A. Ribas, J. M. Timmerman, L. H. Butterfield, J. S. Economou, Determinant spreading and tumor responses after peptide-based cancer immunotherapy. *Trends Immunol* 24, 58-61 (2003).
142. E. Menares *et al.*, Tissue-resident memory CD8(+) T cells amplify anti-tumor immunity by triggering antigen spreading through dendritic cells. *Nat Commun* 10, 4401 (2019).
143. G. Xin *et al.*, Pathogen-Boosted Adoptive Cell Transfer Therapy Induces Endogenous Antitumor Immunity through Antigen Spreading. *Cancer Immunol Res* 8, 7-18 (2020).
144. P. Savas *et al.*, Publisher Correction: Single-cell profiling of breast cancer T cells reveals a tissue-resident memory subset associated with improved prognosis. *Nat Med* 24, 1941 (2018).
145. H. C. Bosmuller *et al.*, Combined Immunoscore of CD103 and CD3 Identifies Long-Term Survivors in High-Grade Serous Ovarian Cancer. *Int J Gynecol Cancer* 26, 671-679 (2016).
146. A. P. Ganesan *et al.*, Tissue-resident memory features are linked to the magnitude of cytotoxic T cell responses in human lung cancer. *Nat Immunol* 18, 940-950 (2017).
147. E. L. Jackson *et al.*, Analysis of lung tumor initiation and progression using conditional expression of oncogenic K-ras. *Genes Dev* 15, 3243-3248 (2001).
148. G. Germano *et al.*, Inactivation of DNA repair triggers neoantigen generation and impairs tumour growth. *Nature* 552, 116-120 (2017).